Egypt. J. Chem. **Vol. 67**, No. 5 pp. 257 - 283 (2024)

Egyptian Journal of Chemistry

http://ejchem.journals.ekb.eg/

In Vitro Evaluation of *Saussurea costus* Gold Nano-Extract as Antioxidant, Anti-Diabetic, Anti-Alzheimer, and Anti-Inflammatory Agent

Amal Gouda Hussien[a], Wael Mahmoud Aboulthana[a*], Ahmed Mahmoud Youssef[b]

[a]*Biochemistry Department, Biotechnology Research Institute, National Research Centre, 33 El Bohouth St. (former El Tahrir St.), Dokki, Giza, P.O. 12622, Egypt*

[b]*Packaging Materials Department, National Research Centre, 33 El Bohouth St. (former El Tahrir St.), Dokki, Giza, P.O. 12622, Egypt*

Abstract

Saussurea costus is rich in numerous aromatic functional groups containing polyphenolic compounds, which possess a wide range of biological properties. The present study focused on utilizing *S. costus* extract for the green synthesis of gold nanoparticles (Au-NPs), which were subsequently used for *in vitro* biological activities.

The extraction process involved the use of 3 different solvents. It was observed that the methanolic *S. costus* extract had the highest concentration of major phyto-constituents, and consequently, demonstrated the highest *in vitro* biological activities. Consequently, it was chosen for the biosynthesis of the Au-NPs, which were characterized using various instrumental techniques. The incorporation of Au-NPs enhanced the biological efficiency compared to the native methanolic extract. Moreover, the gold *S. costus* nano-extract exhibited the lowest median inhibitory concentration (IC_{50}) against human hepatocellular carcinoma (HepG2) cell lines. Treatment of the HepG2 cells with the nano-extract ameliorated the expression of apoptotic genes (EGFR, Bcl-2, and Casp3) compared to the native extract. Furthermore, the gold nano-extract was safer than the native extract when administered orally, as evidenced by the highest median lethal (LD_{50}) and therapeutic doses. The study concluded that the *in vitro* biological activities and safety of the methanolic *S. costus* extract increased after incorporating Au-NPs compared to the native extract.

Keywords*: Saussurea costus*; Green Nanotechnology; Gold Nanoparticles (Au-NPs); Biological Activities; Gene Expression

1. Introduction

Since ancient times, alternative medicine has been recognized as a significant source of remedies, particularly those derived from medicinal plants. Modern medicine, however, faces a challenge in its inability to prevent the onset of diseases. As a result, there is an urgent need to explore the vast resources of nature **[1]**. Numerous medicinal plants have been discovered and studied for their ability to produce a wide range of active chemical compounds that play a crucial role in treating various chronic diseases, including cancer **[2]**. It is widely acknowledged that plants are abundant in natural antioxidants, which effectively reduce the harmful effects caused by oxidative stress **[3]**.

Saussurea costus, also known as *Saussurea lappa*, is a valuable medicinal plant used for treating various conditions such as tenesmus, dyspepsia, diarrhea, vomiting, inflammation, asthma, bronchitis, cough, throat infections, inflammatory diseases, ulcers, and stomach disorders. It also exhibits antiviral activity. Studies by **Tousson et al. [4,5]** and **Ansari et al. [6]** have confirmed its medicinal properties. **Hassan and Masoodi [7]** found that *S. costus* is rich in phyto-constituents like terpenes, anthraquinones, alkaloids, and flavonoids, as well as dehydrocostus lactone and costunolide, which possess various biological properties. These constituents contribute to its anti-diabetic, anti-hypertensive, anti-hepatotoxic, immunostimulant, anthelmintic, anti-inflammatory, anti-tumor, anti-

*Corresponding author e-mail: wmkamel83@hotmail.com)

Receive Date: 27 October 2023, Revise Date: 07 December 2023, Accept Date: 25 December 2023

DOI: 10.21608/EJCHEM.2023.244987.8786

ulcer, antimicrobial, and antifungal effects, as reported by **Ghasham et al. [8]** and **Nadda et al. [9]**.

The methanolic extract of *S. costus* root showed significant antioxidant activity, which can be attributed to its high concentrations of phenols and flavonoids **[10]**. The presence of various functional groups in these secondary metabolites is responsible for their positive biological effects **[11]**. As a result, **Deabes et al. [12]** conducted a study to evaluate the effectiveness of this plant extract in mitigating the hepato- and neurotoxicity induced by chloropyrifos in rats.

Nanotechnology is a prominent field of scientific research that focuses on the synthesis and design of particle structures **[13,14]**. Nanomaterials, with their attractive properties such as stability and the ability to modify their surfaces, have a wide range of applications in advanced biotechnology **[15,16]**. The shapes and sizes of nanoparticles (NPs) play a crucial role in enhancing their chemical, physical, optical, and electrical features **[17]**.

The various metal nanoparticles (M-NPs) prepared using physical and chemical methods have been found to be environmentally unfriendly **[18]**. As a result, the green synthesis of M-NPs has emerged as an alternative approach to conventional methods, particularly in biological research. This method offers several advantages over chemical synthesis, including its suitability for developing biological processes and its potential for large-scale production **[19,20]**. The fabrication of gold nanoparticles (Au-NPs) is particularly important due to their applications in optics, electronics, and human contact. To achieve this in an eco-friendly, cost-effective, and safer manner, researchers have utilized plant extracts, agricultural waste, macroalgae, and macrofungi as stabilizing and reducing agents for biogenic synthesis of Au-NPs using green nanotechnology **[21,22]**.

The present study aimed to explore the use of *S. costus* extract, which contains polyphenolic compounds with aromatic functional groups, for the green synthesis of Au-NPs. Additionally, various instrumental techniques were employed to characterize the biosynthesized Au-NPs. Furthermore, this article evaluated the *in vitro* biological efficacy of the biosynthesized Au-NPs and their impact on the expression of apoptotic genes in human cancer cells.

2. Materials and Methods

2.1. Preparation of different plant extracts

The dried *S. costus* powder was percolated at a concentration of 10% using different solvents (aqueous, methanol, and ethyl acetate) at room temperature, following the method described by **Deabes et al. [12]**. Each extract was macerated for 72 hours, filtered three times, and then evaporated under vacuum using a rotary evaporator, following the procedure suggested by **Akhtar et al. [23]**.

2.2. Quantitative determination of major phyto-constituents

The concentration of total polyphenolic compounds in various plant extracts (aqueous, methanolic, and ethyl acetate) was determined as mg gallic acid/100 gm using the method described by **Singleton and Rossi [24]**. The total tannin content was assessed using tannic acid as a reference compound, following the method proposed by **Broadhurst and Jones [25]**. These assays were repeated in the most effective extract after incorporating Au-NPs.

2.3. *In vitro* biological activities

The biological activities of various plant extracts were assessed, and subsequently, the most effective extract was selected for the biosynthesis of Au-NPs. All analyses were conducted thrice for accuracy and reliability.

2.3.1. Antioxidant activity

The total antioxidant capacity (TAC) was measured in mg gallic acid/gm by analyzing the green phosphate/Mo^{5+} complex at a wavelength (λ) of 695 nm, following the procedure described by **Prieto et al. [26]**. 0.1 ml aliquots of samples were mixed with 1 ml of reagent solution containing 0.3 N sulfuric acid, 28 mM sodium phosphate, and 4 mM ammonium molybdate. Methanol (80%) was used in place of the sample for the blank. The tubes were sealed and incubated in a boiling water bath for 90 minutes. After cooling to room temperature, the absorbance was measured at 695 nm against the blank. The antioxidant capacity was expressed as mg gallic acid equivalent per gram dry weight. All samples were analyzed in triplicate.

The iron reducing power was determined in µg/mL using the method proposed by **Oyaizu [27]**, with

ascorbic acid as the standard. In short, 1ml of the tested extract (1mg/ml) was combined with 1ml of 200mM sodium phosphate buffer (pH 6.6) and 1ml of 1% potassium ferricyanide. The mixture was then incubated at 50°C for 20 minutes, followed by the addition of 1ml of 10% trichloroacetic acid. After centrifugation at 2000rpm for 10 minutes, the upper layer solution (2.5ml) was mixed with 2.5ml of double deionised water and 1ml of fresh ferric chloride (0.1%). The absorbance was measured at 700nm against a blank prepared without the extract. Ascorbic acid at various concentrations was used as a standard. A high absorbance at 700nm indicates a higher reducing power in the reaction mixture.

2.3.2. Scavenging activity

The ability of each extract to scavenge free radicals was determined. The median inhibitory concentration (IC_{50}) required from the tested extract to inhibit 1,1-Diphenyl-2-picryl-hydrazyl (DPPH) radicals was calculated using the method proposed by **Rahman et al. [28]**. The inhibition percent (%) of the 2,2'-azinobis-(3-ethylbenzothiazoline-6-sulfonic acid) (ABTS) radical was calculated using the method described by **Arnao et al. [29]**. The scavenging activities against DPPH and ABTS radicals were compared to ascorbic acid, which was used as the standard.

2.3.3. Anti-diabetic activity

This assay involved calculating the inhibition percentages (%) of α-amylase and α-glucosidase enzymes. The methods used were based on the techniques demonstrated by **Wickramaratne et al. [30]** for α-amylase inhibition and **Pistia-Brueggeman and Hollingsworth [31]** for α-glucosidase inhibition. Acarbose was used as the standard drug.

For assaying α-amylase inhibition (%), 0.5 ml of the test solution was combined with 0.5 ml of α-amylase solution (0.5 mg/ml) and buffer (Na_2HPO_4/NaH_2PO_4 (0.02 M), NaCl (0.006 M) at pH 6.9) to create concentrations ranging from 25 to 800 µg/mL. The mixture was then left at room temperature for 10 minutes before adding 200 µL of starch solution (1% in water (w/v) buffer (Na_2HPO_4/NaH_2PO_4 (0.02 M), NaCl (0.006 M) at pH 6.9)). The reaction was stopped by adding 200 µL of DNSA (coloring) reagent (12 g of sodium potassium tartrate tetrahydrate in 8.0 mL of 2 M NaOH and 20 mL of 96 mM of DNSA solution). The test tubes were then placed in a boiling water bath (100 °C) for 10 minutes and the mixture was cooled to room temperature and diluted with 5 mL of distilled water. The absorbance was measured at 540 nm using a UV-Visible spectrophotometer.

The α-glucosidase inhibition (%)was estimated by incubating the extract (50 µL) with 10 µL of the α-glucosidase enzyme solution (1 U/mL) for 20 min at 37 °C with an additional 125 µL of 0.1 M phosphate buffer (pH 6.8). After 20 minutes, the reaction was started with the addition of 20 µL of 1 M p-nitrophenyl-α-D-glucopyranoside (pNPG) (substrate), and the mixture was incubated for 30 minutes. The reaction was terminated with the addition of 50 µL of Na_2CO_3 (0.1 N), and final absorbance was measured at 405 nm.

2.3.4. Anti-Alzheimer's activity

In this assay, the percentage of inhibition of the acetyl cholinesterase (AChE) enzyme was evaluated using Ellman's method **[32]**, with donepezil as the standard drug.

The tested extract was dissolved in a 0.1 M phosphate buffer at pH 8. For each run, 5 µl of Acetylthiocholine (ATCh) at a concentration of 0.5 mM, 5 µl of 5,5'-dithiobis-2-nitrobenzoic acid (DTNB) at a concentration of 0.03 mM, and 5 µl of the tested sample solution at various concentrations were added to a flat bottom 96-well plate. The mixture was then incubated for 10 minutes at 30°C. After incubation, 5 µl of AChE at a concentration of 0.3 U/ml was added to start the reaction, and the absorbance was measured at 412nm. A control run was also performed, which included all the components except for the test extract. All experiments were conducted in triplicate.

2.3.5. Anti-inflammatory activity

This assay involved the determination of protein denaturation (%) **[33]** and proteinase inhibition **[34]** using diclofenac sodium as the standard non-steroidal anti-inflammatory drug, as prepared according to **Meera et al. [35]**.

The protein denaturation (%) was measured by mixing the test control solution (0.5ml) was prepared by mixing 0.45 ml bovine serum albumin (BSA) (5% w/v aqueous solution) with 0.05 ml distilled water. The test solution (0.05 ml) added to 0.45 ml distilled water to form the product control (0.5 ml). The different extracts (test solution) and

diclofenac sodium (standard) were used. The pH value in all prepared solutions was adjusted to 6.3 using HCl (1N). All the samples were incubated at 37 ^{o}C for 20 min and the temperature increased to 57 ^{o}C and the samples were maintained at that degree for 3 min. Phosphate buffer (2.5 ml) was added to the prepared solutions after cooling. The absorbance was determined at 416 nm using a UV-Visible spectrophotometer. Percentage of protein denaturation inhibition can be calculated.

Proteinase inhibitory activity was determined by adding the test sample (1 ml) to a reaction mixture consisting of 0.06 mg trypsin dissolved in 1 ml of 20 mM Tris HCl buffer (pH 7.4). After incubating the mixture for 5 minutes at 37°C, 1 ml of casein (0.8% w/v) was added. It was then incubated for an additional 20 minutes, followed by the addition of 2 ml perchloric acid (70%) to terminate the reaction. After centrifugation of the cloudy suspension, the absorbance of the supernatant was determined at 210 nm against buffer as the blank, and the percentage of the proteinase inhibitory activity was calculated.

2.3.6 Cytotoxic activity

The efficiency of each extract against human colon (Caco2) and hepatocellular carcinoma (HepG2) cell lines was determined by assaying the optical density (OD) at wavelength 570 using the 3-(4,5-dimethythiazol-2-yl)-2,5-diphenyl tetrazolium bromide (MTT) assay **[36]**. The percentage of cell-growth inhibition (%) and median inhibitory concentration (IC_{50}) were calculated using IC_{50} calculation software.

2.4. Molecular assays

2.4.1. DNA content analysis

The cultured HEGP-2 cells (3×10^5/well) were treated with each extract, fixed, and then incubated with propidium iodide (PI) staining solution (50 ng/mL) and RNA-ase (0.1 mg/mL) in a dark place for 15 minutes. The DNA in the HEGP-2 cells was quantified using flow cytometry (BD FASCCalibur-USA).

2.4.2. Extraction of RNA and quantitative RT-PCR

The cultured HepG2 cells were treated with each extract at a concentration of 100 µg/ml. Total RNAs were extracted from the treated cells using the RNeasy Mini Kit (Qiagen RNA extraction/BioRad syber green PCR MMX) following the method suggested by **Pfaffl [37]**. The extracted RNAs were then used for cDNA synthesis during the reverse transcription process using the High Capacity cDNA Reverse Transcriptase kit (Applied Biosystems, USA). To quantify the levels of EGFR, Bcl-2, and Casp3 gene expressions, the Step One instrument (Applied Biosystems, USA) was used to amplify the cDNA with the Syber Green I PCR Master Kit (Fermentas). The amplification process followed a thermal program consisting of 10 minutes at 95 ºC for enzyme activation, followed by 40 cycles of 15 seconds at 95 ºC, 20 seconds at 55 ºC, and 30 seconds at 72 ºC. The ΔCt method was used to normalize the changes in expression of each target gene relative to the mean critical threshold (CT) values of the housekeeping gene (GAPDH). For each target gene, specific primers (1µl) were added: EGFR (F: 5'-GACTCCGTCCAGTATTGATCG-3'; B: 5'-GCCCTTCGCACTTCTTACACTT-3'), Bcl2 (F: 5'-TCCCTCGCTGCACAAATACTC-3'; B: 5'-ACGACCCGATGGCCAAGA-3'), Casp3 (F: 5'-TGTTTGTGTGCTTCTGAGCC-3'; B: 5'-CACGCCATGTCATCATCAAC-3'), and GAPDH (F: 5'-GAAGGTGAAGGTCGGAGTCA-3'; B: 5'-TTGAGGTCAATGAAGGGGTC-3'). The 2-ΔΔCq method, as suggested by **Wang et al. [38]**, was used to quantify the levels of mRNA expression. The results for each target gene were calculated from triplicate experiments.

2.5. Cell apoptosis

The HepG2 cells (3×10^6/well) were cultured overnight and then treated with each extract at concentrations of 50, 100, 150, and 200 µg/ml. Additionally, the tested extract was added to the cultured HepG2 cells at a concentration of 100 µg/ml and at different time points (24, 36, 48, and 72 hrs). The HepG2 cells were collected by cold centrifugation at approximately 300 x g for 10 min, and then 100 µl of 1X Binding Buffer was added per sample. The Annexin V-FITC apoptosis detection kit (Annexin V-FITC-BD Bioscience PharmingenTM, USA) was used to assess cell apoptosis. Annexin V (100 µl) was incubated with treated HepG2 cells (10^6 cells/ml). Annexin V-FITC (5 µl) and PI (5 µl) were incubated in a dark place for 15 min, followed by the addition of 400 µl

of binding buffer (1X). The flow cytometry (BD FASCCalibur-USA) was immediately used to analyze the HepG2 cells for a maximal signal within 1 hr, as suggested by **Koopman et al. [39]**.

2.6. Biosynthesis of gold nanoparticles (Au-NPs)

2.6.1. Preparation of gold plant nano-extract

The fabrication of Au-NPs was conducted in two main steps using the chemical reduction method as described by **Zhao et al. [40]**. In Part I, Au^{+3} ($HAuCl_4$) was reduced to Au0 through a reaction in an aqueous solution containing trisodium citrate ($Na_3C_6H_5O_7.2H_2O$). Part II focused on stabilizing the Au-NPs to prevent particle aggregation, which was achieved by using cetyltrimethylammonium bromide (CTAB).

The spontaneous emulsification method was used to prepare a nano-emulsion. The dried methanolic extract was mixed with Tween 20 (a non-ionic surfactant), cellulose nanocrystal (CNC), and water in two steps. In the first step, the organic phase was created by mixing the dried extract with Tween 20. Then, CNC (3 gm) was added, followed by sonication for 30 minutes. During the second step, the organic phase containing the plant extract, Tween 20, and CNC was gradually added to water using a separating funnel, drop by drop (20 mL/min). The mixture was then stirred for 5 hours at 800 rpm. To this nanoemulsion, the prepared Au-NPs were added at a concentration of 1% and sonicated for 30 minutes at 50 °C.

2.6.2. Characterization of the biosynthesized Au-NPs

The spectrum of the biosynthesized Au-NPs was assessed by diluting it 10-fold with deionized water. The assessment was done using a Shimadzu UV-VIS recording spectrophotometer UV-240, with a wavelength range of 200 to 800nm. To analyze the crystalline nature and size of the biosynthesized Au-NPs, a Philips X-ray diffractometer (XRD) was used. The XRD was equipped with an X-ray source (Cu Kα radiation) with the following specifications: 45 kV, 40 mA, and a wavelength of 0.15418 nm. The morphological nature of the biosynthesized Au-NPs, including their shapes and sizes, was measured using a transmission electron microscope (TEM). The specific model used was JEM-1230 from Japan. The analysis was carried out at a resolution of up to 0.2 nm, with a maximum magnification of $600X10^3$, and a high resolution level of 200 KV.

2.7. Median lethal dose (LD_{50})

One hundred and sixty (160) adult albino mice weighing between 20-25 g were divided into 16 groups, with 10 mice in each group. Seven groups were orally treated with increasing doses (1000, 2000, 4000, 6000, 8000, 10000, and 12000 µg/Kg) to determine the LD_{50} of the native extract. The remaining nine groups were treated with increasing doses (1000, 2000, 4000, 6000, 8000, 10000, 12000, 14000, and 16000 µg/Kg) to determine the LD_{50} of the gold nano-extract. The LD_{50} was calculated by counting the number of dead mice after 24 hours of oral administration, using the equation proposed by **Paget and Barnes [41]**.

3. Results

3.1. Quantitative determination of the major phyto-constituents

During the current study, the polyphenolic compounds and tannins were quantified in the plant extracts prepared using different organic solvents (aqueous, methanolic, and ethyl acetate) because they are the major active phyto-constituents.

The results of the total polyphenolic and tannin contents, as well as the TAC and IRP of different plant extracts, are presented in **Table 1**. It was observed that the total methanolic extract had the highest concentrations of total polyphenolic (154.99±0.10 mg gallic acid/100 gm) and tannin contents (37.28±0.02 µg/mL). The antioxidant activity of the extracts was found to be directly related to the concentrations of these phyto-constituents. Consequently, the total methanolic extract exhibited the highest values of TAC and IRP (172.01±0.11 mg gallic acid/gm; 156.73±0.04 µg/mL, respectively).

3.2. *In vitro* biological activities of different plant extracts

The biological activities of various plant extracts were evaluated by measuring their scavenging activities against DPPH and ABTS radicals. Ascorbic acid was used as a standard for comparison. Additionally, the extracts were tested for their anti-diabetic, anti-Alzheimer's, and anti-inflammatory activities. The scavenging activity against DPPH radicals was quantified using IC_{50} values, with lower values indicating stronger antioxidant activity.

Thus, the extract with the lowest IC_{50} value exhibited the highest scavenging activity against DPPH radicals. In terms of ABTS radicals, the scavenging activity was determined by the highest inhibitory percentage. The data presented in **Table 2** demonstrated that the total methanolic extract displayed the highest scavenging activities against DPPH radicals (IC_{50}=7.35±0.02 µg/ml) and ABTS (25.27±0.03%) compared to the other extracts.

The anti-diabetic activity of the extracts was assayed by determining their inhibitory effect on α-amylase and α-glucosidase enzymes using acarbose as a standard drug. The highest inhibitory effects against the activities of α-amylase (41.70±0.03%) and α-glucosidase (38.17±0.01%) were noticed with the total methanolic extract, indicating the highest anti-diabetic activity. The anti-Alzheimer's activity of the different extracts was assayed by measuring their inhibitory effect against the activity of AChE enzyme. It possessed the highest inhibitory effect against the activity of AChE (26.18±0.01%), indicating the highest anti-Alzheimer's activity compared to the other native plant extracts using donepezil as a standard. Regarding anti-inflammatory activity, the efficiency of the different extracts was assayed by determining their inhibitory effect on protein denaturation and proteinase activity. The highest inhibitory effects on proteinase denaturation (30.48±0.02%) and proteinase (28.77±0.01%) were noticed with the total methanolic extract compared to the other extracts. Therefore, it possessed the highest anti-inflammatory activity compared to diclofenac sodium that was used as a standard.

3.3. The structural properties of the biosynthesized Au-NPs

The total methanolic extract was chosen for the green synthesis of Au-NPs due to the presence of bio-macromolecules (polyphenolic and condensed tannins) that have strong antioxidant capacity. The UV-Vis spectroscopy data **(Fig. 1a)** showed a sharp peak at 500 nm, indicating the presence of biosynthesized Au-NPs. To determine the structural properties of the biosynthesized Au-NPs, XRD and TEM techniques were used. The XRD diffraction pattern **(Fig. 1b)** revealed diffraction peaks similar to those of metallic Au phase (AuCl4-), with the most significant peaks at 38°, 43.8°, and 65° corresponding to the crystallographic planes (1 1 1), (2 0 0), and (2 2 0) respectively. TEM analysis **(Fig. 1c)** showed that the biosynthesized Au-NPs had an average width of 19 nm, with some particles of lower and higher size distribution. The shapes of the Au-NPs were predominantly spherical or round.

3.4. The phyto-constituents in the extract incorporated with Au-NPs

Data presented in **Table 3** demonstrates that the concentration of total polyphenolic compounds (251.08±0.17 mg gallic acid/100 gm) and total tannin content (60.40±0.03 µg/mL) increased following the incorporation of Au-NPs. The antioxidant activity is directly influenced by the concentration of these phyto-constituents. Consequently, the TAC and IRP levels increased in the gold nano-extract (278.65±0.18 mg gallic acid/gm; 253.91±0.06 µg/mL, respectively), surpassing those found in the native extract itself (172.01±0.11 mg gallic acid/gm; 156.73±0.04 µg/mL, respectively).

3.5. *In vitro* biological activities of the extract incorporated with Au-NPs

Data presented in **Table 4** demonstrated that the gold nano-extract exhibited the highest biological activity (4.535±0.01 µg/ml) compared to the native extract (7.35±0.02 µg/ml). The IC_{50} of the standard ascorbic acid was determined to be 4.10±0.01 µg/mL. In terms of scavenging activity against ABTS radical, at an equal concentration of 100 µg/mL, the gold nano-extract (40.94±0.04%) displayed a higher inhibitory effect against ABTS radical compared to the native extract (25.27 ± 0.03%). The inhibitory effect of ascorbic acid (standard) at the same concentration was 39.10±0.01%.

At equal concentrations of the native extract and gold nano-extract, it was observed that the gold nano-extract had a higher inhibitory effect on α-amylase and α-glucosidase activities (67.56±0.05% and 61.84±0.02%, respectively) compared to the native extract (41.70±0.03% and 38.17±0.01%, respectively). In contrast, at the same concentration, the standard acarbose showed an inhibitory effect of 77.43±0.01% and 55.79±0.01% on the activity of α-amylase and α-glucosidase enzymes, respectively.

Table 1
Major active phyto-constituents and antioxidant activity of different *S. costus* extracts.

	Active Phyto-constituents		Antioxidant Activity	
	Total Polyphenols (mg gallic acid/100 gm)	**TCT (µg/ml)**	**TAC** (mg gallic acid/gm)	**IRP (µg/mL)**
Aqueous	96.87 ± 0.06	23.30 ± 0.01	107.50 ± 0.07	97.96 ± 0.02
Methanolic	**154.99 ± 0.10**	**37.28 ± 0.02**	**172.01 ± 0.11**	**156.73 ± 0.04**
EtOH	82.44 ± 0.05	19.83 ± 0.01	91.49 ± 0.06	83.37 ± 0.02

Values were expressed as mean ± standard error (SE) of three replicates.

Table 2
Comparing the major biological activities of various *S. costus* extracts with standard substances.

	Scavenging Activity		Inhibition (%)			Anti-inflammatory Activity	
			Anti-diabetic Activity		Anti-Alzheimer Activity		
	DPPH (IC_{50} µg/ml)	**ABTS** (%)	**α-Amylase**	**α-Glucosidase**	**AChE**	**Proteinase Denaturation** (%)	**Inhibition of Proteinase** (%)
Aqueous	11.75 ± 0.03	15.79 ± 0.02	33.10 ± 0.02	30.30 ± 0.01	23.80 ± 0.01	27.71 ± 0.02	26.16 ± 0.01
Methanolic	**7.35 ± 0.02**	**25.27 ± 0.03**	**41.70 ± 0.03**	**38.17 ± 0.01**	**26.18 ± 0.01**	**30.48 ± 0.02**	**28.77 ± 0.01**
EtOH	13.81 ± 0.04	13.44 ± 0.01	27.08 ± 0.02	24.78 ± 0.01	21.81 ± 0.01	25.40 ± 0.01	23.98 ± 0.01
STD	**Ascorbic Acid**		**Acarbose**		**Donepezil**	**Diclofenac Sodium**	
	4.10 ± 0.01	39.10 ± 0.01	77.43 ± 0.01	55.79 ± 0.01	69.00 ± 0.04	48.54 ± 0.01	45.79 ± 0.01

Values were expressed as mean ± standard error (SE) of three replicates.

Table 3
The major active phyto-constituents and antioxidant activity of the total methanolic extract of *S. costus* incorporated with Au-NPs and compared to native extract.

	Active Phyto-constituents		Antioxidant Activity	
	Total Polyphenols (mg gallic acid/100 gm)	TCT (µg/ml)	TAC (mg gallic acid/gm)	IRP (µg/mL)
Native Ext.	154.99 ± 0.10	37.28 ± 0.02	172.01 ± 0.11	156.73 ± 0.04
Gold Nano-Ext.	251.08 ± 0.17	60.40 ± 0.03	278.65 ± 0.18	253.91 ± 0.06

Values were expressed as mean ± standard error (SE) of three replicates.

Table 4
The major biological activities of the total methanolic extract of *S. costus* incorporated with Au-NPs and compared to native extract.

	Scavenging Activity		Inhibition (%)			Anti-inflammatory Activity	
			Anti-diabetic Activity		Anti-Alzheimer Activity		
	DPPH (IC_{50} µg/ml)	ABTS (%)	α-Amylase	α-Glucosidase	AChE	Proteinase Denaturation (%)	Inhibition of Proteinase (%)
Native Ext.	7.35 ± 0.02	25.27 ± 0.03	41.70 ± 0.03	38.17 ± 0.01	26.18 ± 0.01	30.48 ± 0.02	28.77 ± 0.01
Gold Nano-Ext.	4.535 ± 0.01	40.94 ± 0.04	67.56 ± 0.05	61.84 ± 0.02	26.18 ± 0.02	30.49 ± 0.01	28.78 ± 0.02
STD	Ascorbic Acid		Acarbose		Donepezil	Diclofenac Sodium	
	4.10 ± 0.01	39.10 ± 0.01	77.43 ± 0.01	55.79 ± 0.01	69.00 ± 0.04	48.54 ± 0.01	45.79 ± 0.01

Values were expressed as mean ± standard error (SE) of three replicates.

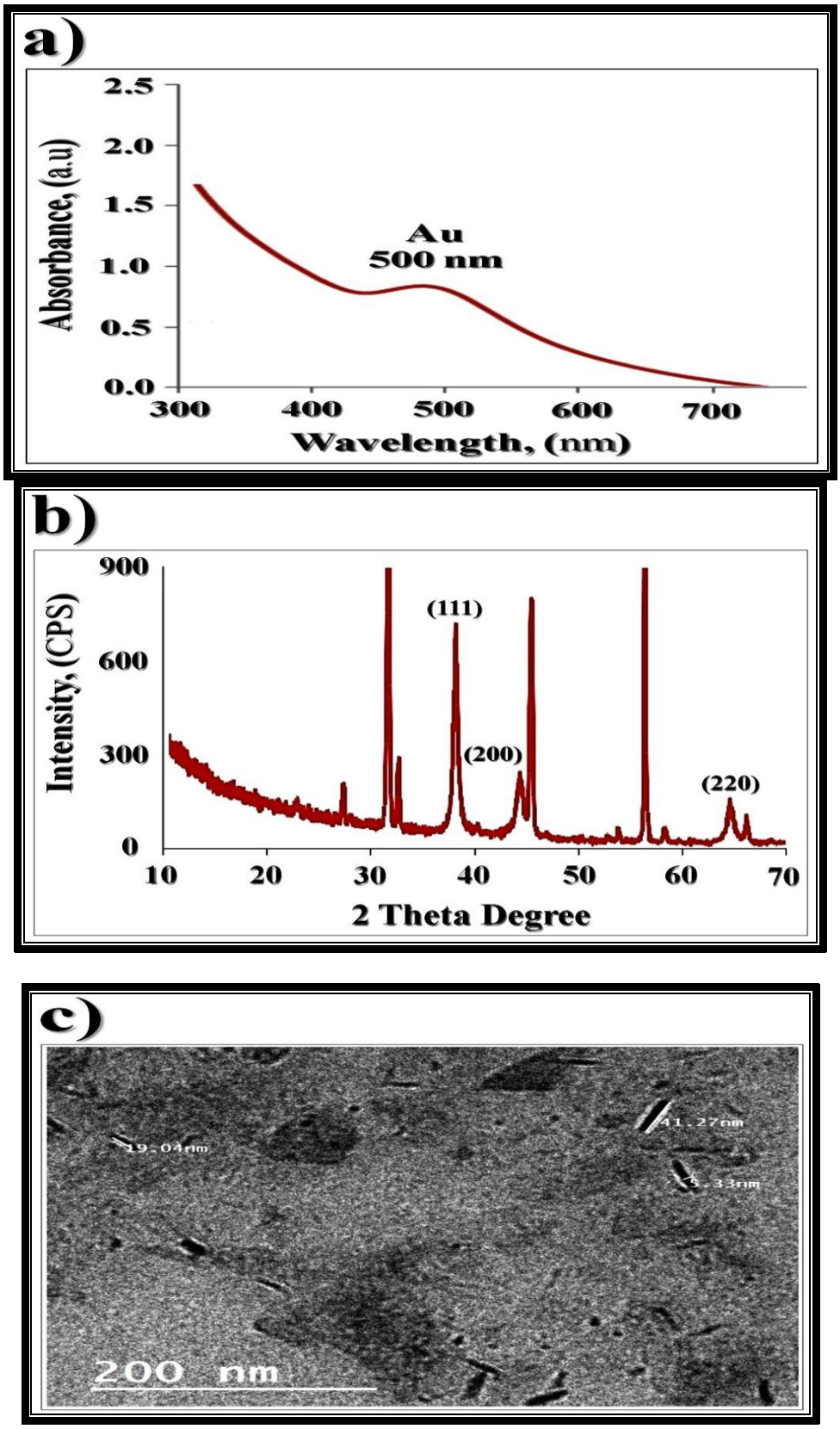

Figure 1: The biosynthesized gold nanoparticles (Au-NPs) were characterized using **a)** Ultraviolet-visible (UV-VIS) spectrum, **b)** X-Ray Diffraction (XRD) spectrum, **c)** Transmission Electron Microscope (TEM) image.

It was discovered that both the native extract and gold nano-extract had the same effect on AChE activity at equal concentrations (26.18±0.01% and 26.18±0.02%, respectively). In comparison, the standard drug Donepezil had an inhibitory effect of 69.00 ± 0.04% on AChE activity at the same concentration.

Regarding anti-inflammatory activity, it was discovered that both the native extract and gold nano-extract demonstrated similar inhibitory effects on proteinase denaturation (30.48±0.02 and 30.49±0.01, respectively) and proteinase activity (28.77±0.01 and 28.78±0.02, respectively). In comparison, at the same concentration, diclofenac sodium (standard) exhibited inhibitory effects on proteinase denaturation of 48.54±0.01 and 45.79±0.01, respectively.

As depicted in **Figure 2**, the methanolic extract combined with Au-NPs exhibited the most potent *in vitro* cytotoxic activity against Caco2, with the lowest IC_{50} value recorded at 41.33 µg/mL. This was followed by the native extract, which had an IC_{50} value of 63.33 µg/mL.

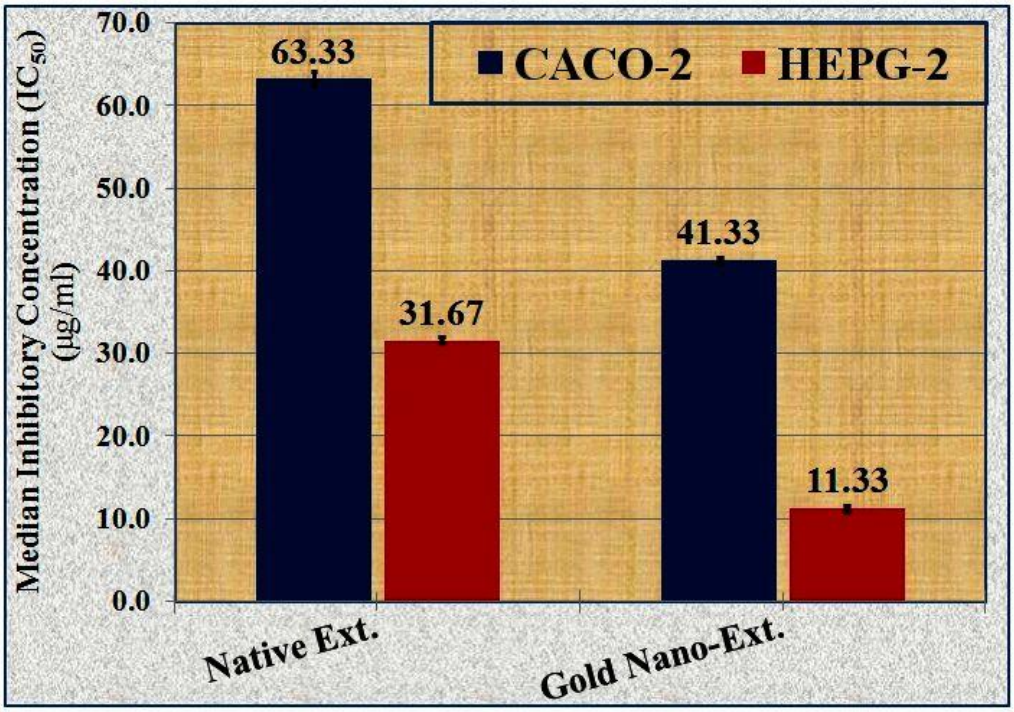

Figure 2: The median inhibitory concentrations (IC_{50}) of methanolic *S. costus* extract incorporated with Au-NPs against human colon (Caco2) and liver cancer (HepG2) cell line and compared to the native extract.

Figure 3 illustrates the shapes and distribution of Caco2 cells treated with the native extract and gold nano-extracts at the median (IC_{50}) and maximum inhibitory concentration (100 µg/mL), in comparison to the control Caco2 cells (at a concentration of 0 µg/mL). Regarding HepG2 cells, the gold nano-extract demonstrated the highest cytotoxic activity, with an IC_{50} value of 11.33 µg/mL, followed by the native extract with an IC_{50} value of 31.67 µg/mL **(Figure 2)**.

Figure 4 displays the shapes and distribution of HepG2 cells treated with the native extract and gold nano-extracts at the median (IC_{50}) and maximum inhibitory concentration (100 µg/mL), in comparison to the control HepG2 cells (at a concentration of 0 µg/mL).

The results of this study indicated that the methanolic extract, both before and after incorporating Au-NPs, exhibited greater cytotoxic activity against HepG2 cells compared to Caco2 cells. As a result, additional investigations were conducted on HepG2 cells to assess the effectiveness of the extracts in influencing the expression of specific genes at the molecular level.

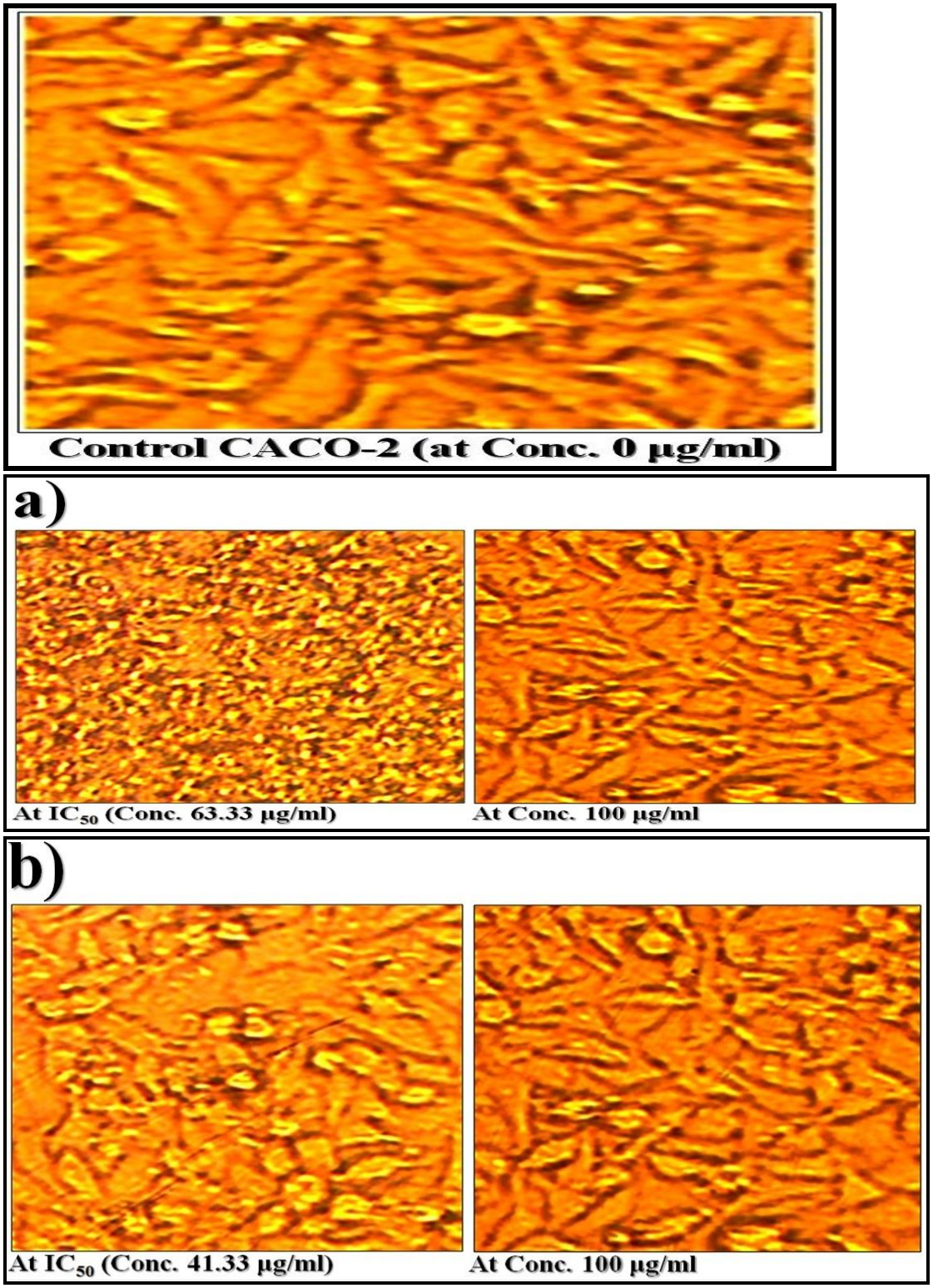

Figure 3: The median (IC_{50}) and maximum (Conc. 100 µg/ml) inhibitory concentrations of methanolic *S. costus* extract a) before incorporating Au-NPs, b) after incorporating Au-NPs against human colon cancer (Caco2) cell line and compared to control Caco2.

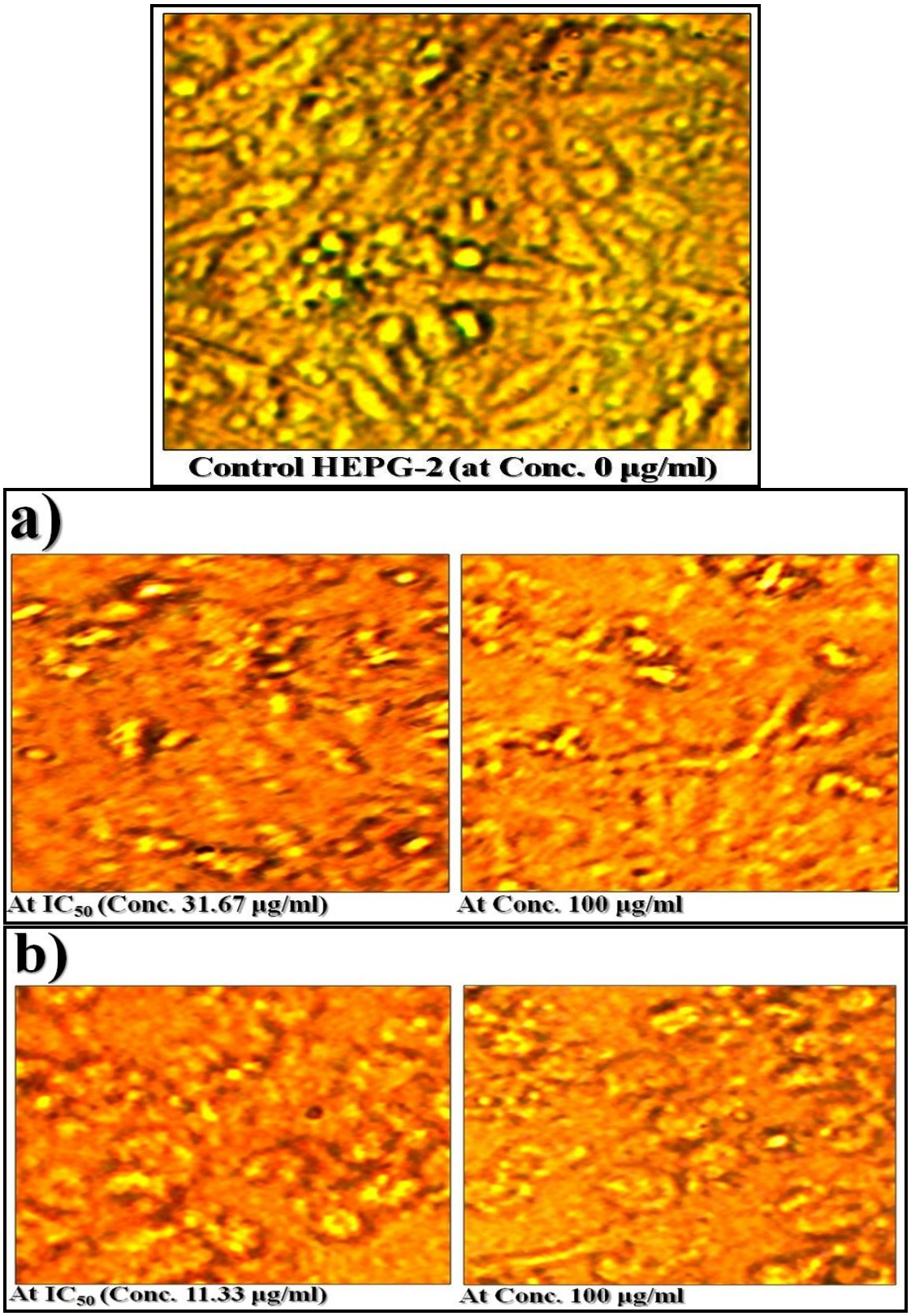

Figure 4: The median (IC_{50}) and maximum (Conc. 100 µg/ml) inhibitory concentrations of methanolic *S. costus* extract **a)** before incorporating Au-NPs, **b)** after incorporating Au-NPs against human liver cancer (HepG2) cell line and compared to control HepG2.

As depicted in **Figure 5**, the fold changes of EGFR and Bcl2 genes exhibited a decrease in HepG2 cells treated with gold nano-extract (0.52 and 0.44, respectively) compared to cells treated with native extract (0.76 and 0.85, respectively). In regards to the Casp-3 gene, its fold changes increased (2.91) in HepG2 cells treated with gold nano-extract compared to cells treated with native extract (1.95). The standard drug DOX reduced the fold changes of EGFR, Bcl2, and Casp-3 genes to 0.17, 0.60, and 8.39, respectively, in comparison to the fold changes observed in the control HepG2 cells.

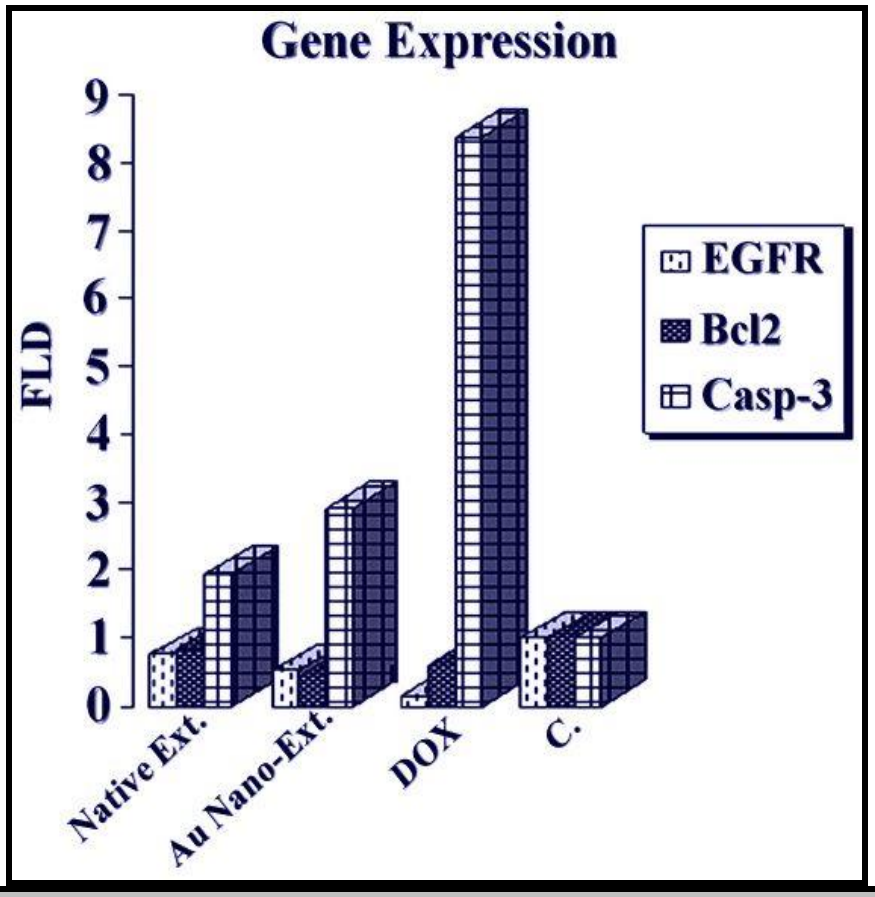

Sample	Gene Expression		
	Fold Change		
	EGFR	Bcl2	Casp-3
Native Extract	0.76	0.85	1.95
Gold Nano-extract	0.52	0.44	2.91
Doxorubicin	0.17	0.60	8.39
Control	1.00	1.00	1.00

Figure 5: Values of the fold change in the EGFR, Bcl2 and Casp-3 genes expressed in the HepG2 cells treated with gold *S. costus* nano-extract and compared to the native extract and doxorubicin (as standard drug).

As shown in **Figure 6**, treatment of HepG2 cells with gold nano-extract resulted in the arrest of cell

growth at the **G2/M** and **Pre-G1** phases. Additionally, there was an increased accumulation of cells at these phases, with percentages of approximately 27.97% and 17.39%, respectively. This was in contrast to the cells treated with native extract or the control HepG2 cells themselves. Conversely, the nano-extract led to a decrease in the accumulation of HepG2 cells at the **G0-G1** and **S** phases, with percentages of approximately 38.07% and 33.96%, respectively. Again, this was in comparison to the cells treated with native extract or the control HepG2 cells themselves.

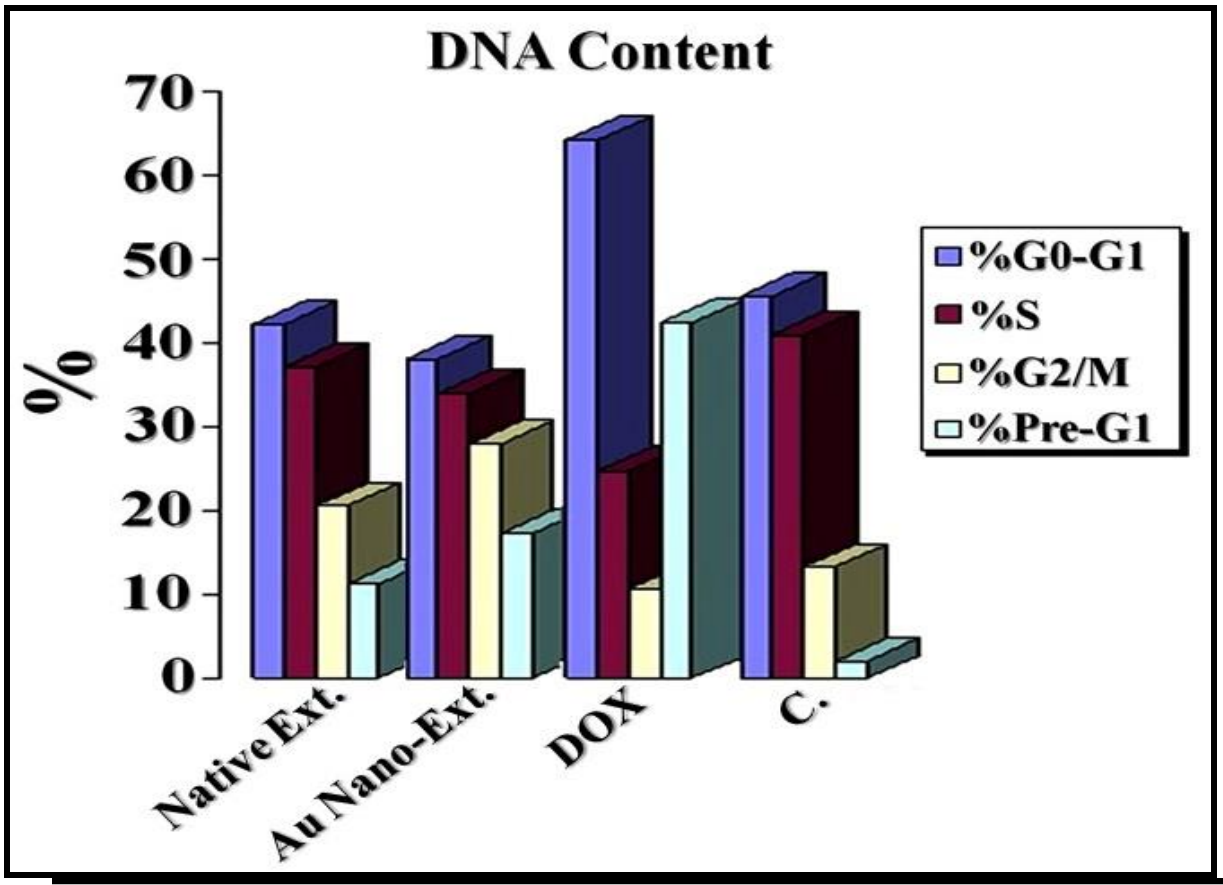

Sample	DNA Content				
	%G0-G1	%S	%G2/M	%Pre-G1	Comment
Native Extract	42.21	37.15	20.64	11.27	Cell growth arrest@G2/M
Gold Nano-extract	38.07	33.96	27.97	17.39	Cell growth arrest@G2/M
Doxorubicin	64.31	24.91	10.78	42.55	Cell growth arrest@G1
Control	45.61	41.08	13.31	2.02	-

Figure 6: Chart showing data of cell cycle analysis in HepG2 cells treated with gold *S. costus* nano-extract and compared to the native extract and doxorubicin (as standard drug).

As shown in **Figure 7**, treatment of HepG2 cells with gold nano-extract increased the percentage of total apoptotic cells (17.39%), as well as early (2.75%) and late apoptotic cells (5.52%), compared to cells treated with the native extract or control HepG2 cells. Additionally, the percentage of necrotic cells was higher in HepG2 cells treated with nano-extract (9.12%) compared to those treated with the native extract (3.51%). The

standard drug DOX also increased the percentage of total apoptotic cells (42.55%), as well as early (3.06%) and late apoptotic cells (27.33%), along with the percentage of necrotic cells (12.16%), compared to cells treated with the native extract or control HepG2 cells.

Flow cytometric analysis data **(Figure 8)** using Annexin V-FITC **(Figure 9)** showed that treatment of HepG2 cells with gold nano-extract enhanced apoptosis compared to cells treated with the native extract or control HepG2 cells. Data depicted in **Table 5** showed no significant changes in the expression of the EGFR, Bcl2, and Casp-3 genes in HepG2 cells treated with the native extract and gold nano-extract compared to cells treated with DOX (standard drug) or control HepG2 cells.

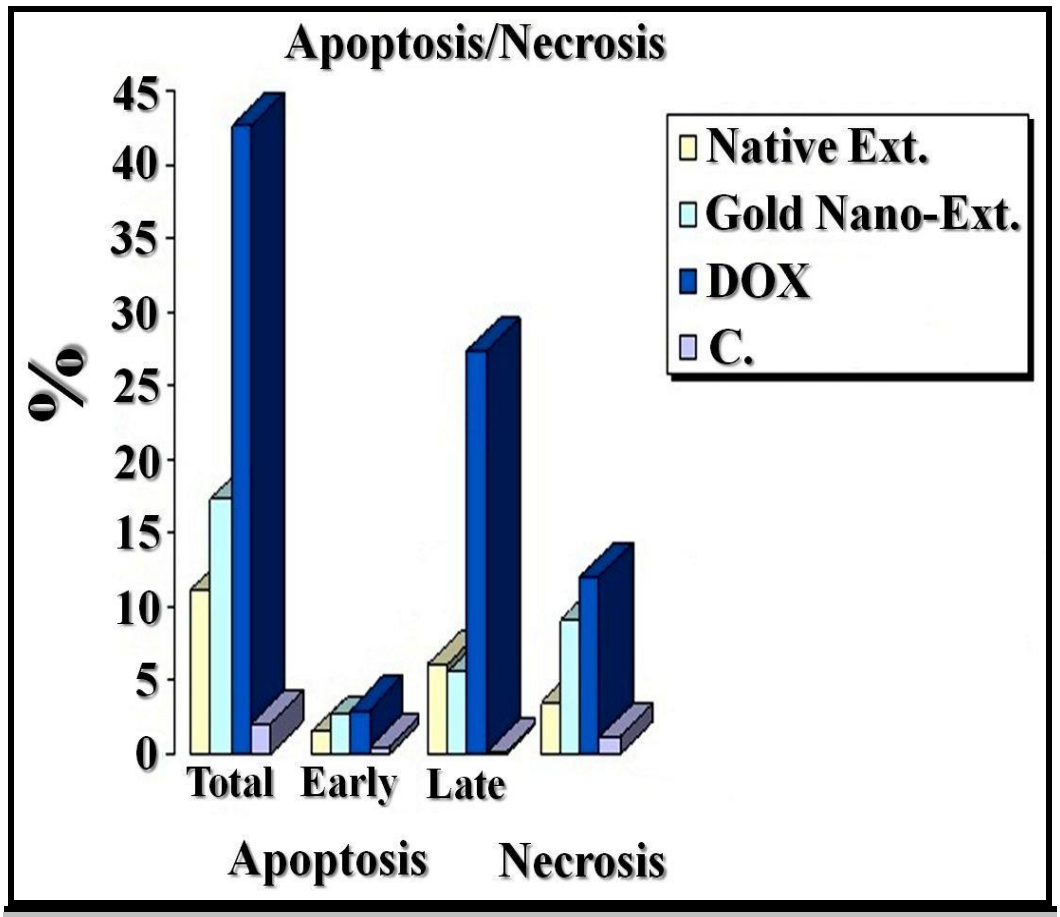

Sample	Apoptosis			Necrosis
	Total	Early	Late	
Native Extract	11.27	1.61	6.15	3.51
Gold Nano-extract	17.39	2.75	5.52	9.12
Doxorubicin	42.55	3.06	27.33	12.16
Control	2.02	0.53	0.24	1.25

Figure 7: Chart showing data of apoptosis in HepG2 cells treated with gold *S. costus* nano-extract and compared to the native extract and doxorubicin (as standard drug).

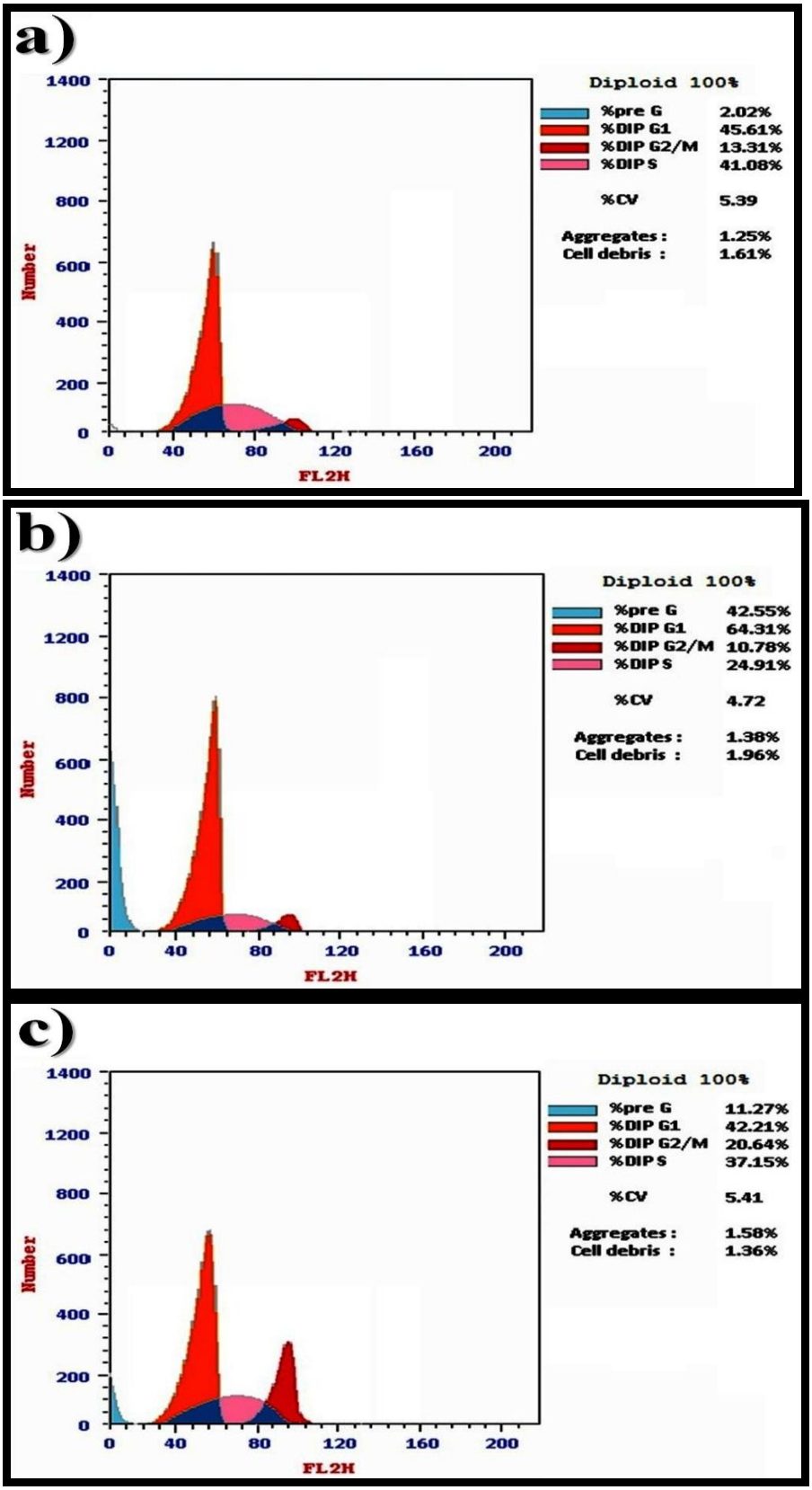
a)
Diploid 100%
%pre G 2.02%
%DIP G1 45.61%
%DIP G2/M 13.31%
%DIP S 41.08%
%CV 5.39
Aggregates : 1.25%
Cell debris : 1.61%
Number
FL2H
b)
Diploid 100%
%pre G 42.55%
%DIP G1 64.31%
%DIP G2/M 10.78%
%DIP S 24.91%
%CV 4.72
Aggregates : 1.38%
Cell debris : 1.96%
Number
FL2H
c)
Diploid 100%
%pre G 11.27%
%DIP G1 42.21%
%DIP G2/M 20.64%
%DIP S 37.15%
%CV 5.41
Aggregates : 1.58%
Cell debris : 1.36%
Number
FL2H

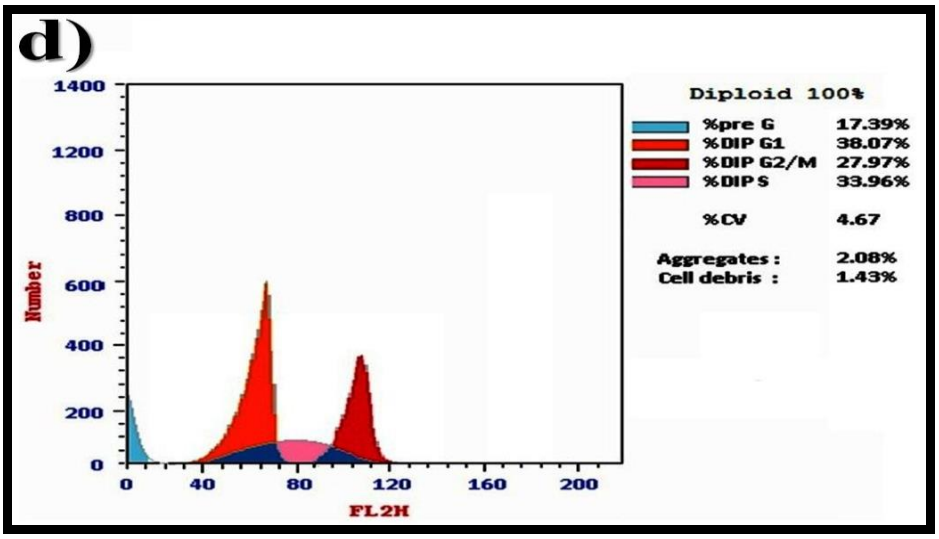

Figure 8: Data of DNA content in a) Control HepG2, b) HepG2 treated with doxorubicin, c) HepG2 treated with native *S. costus* extract, d) HepG2 treated with gold *S. costus* nano-extract.

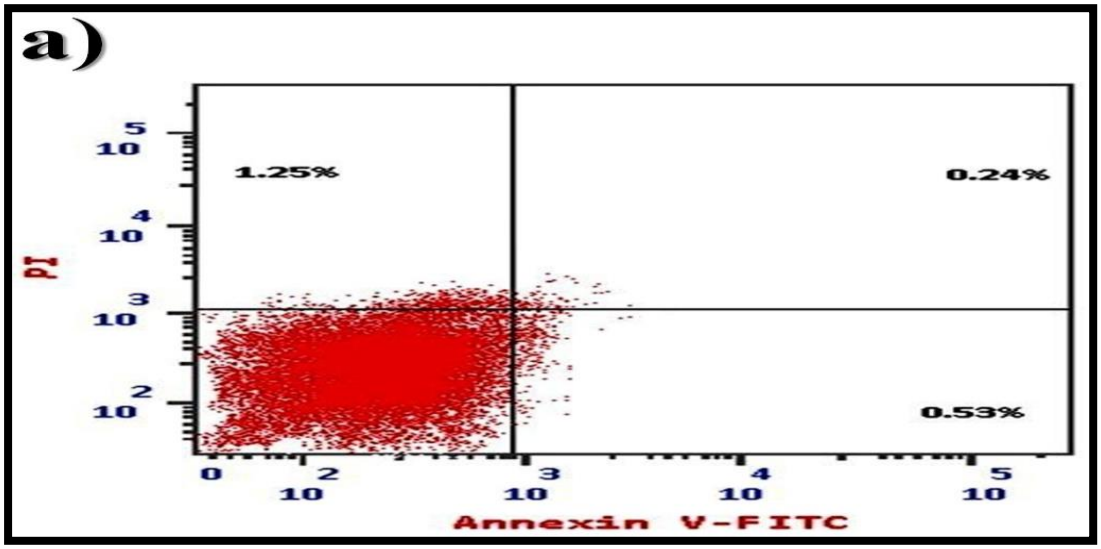

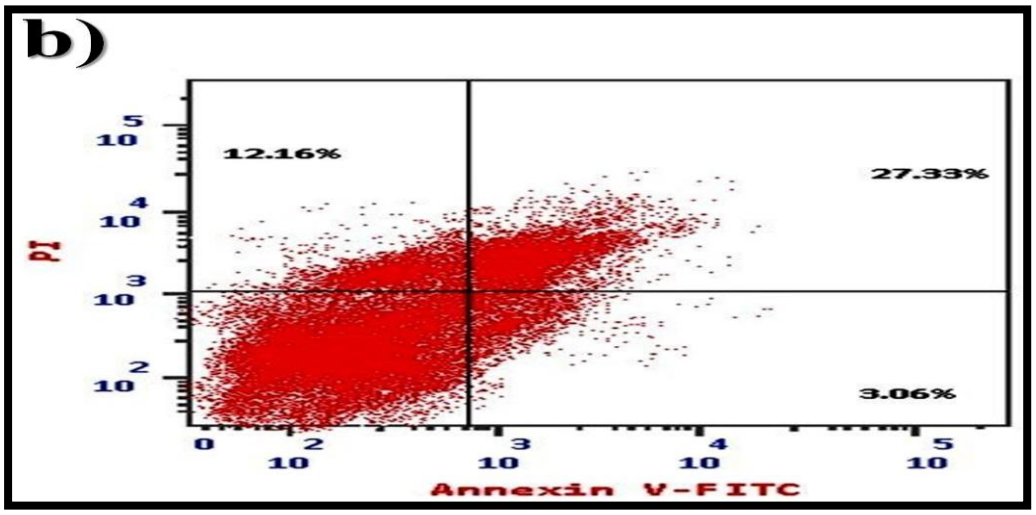

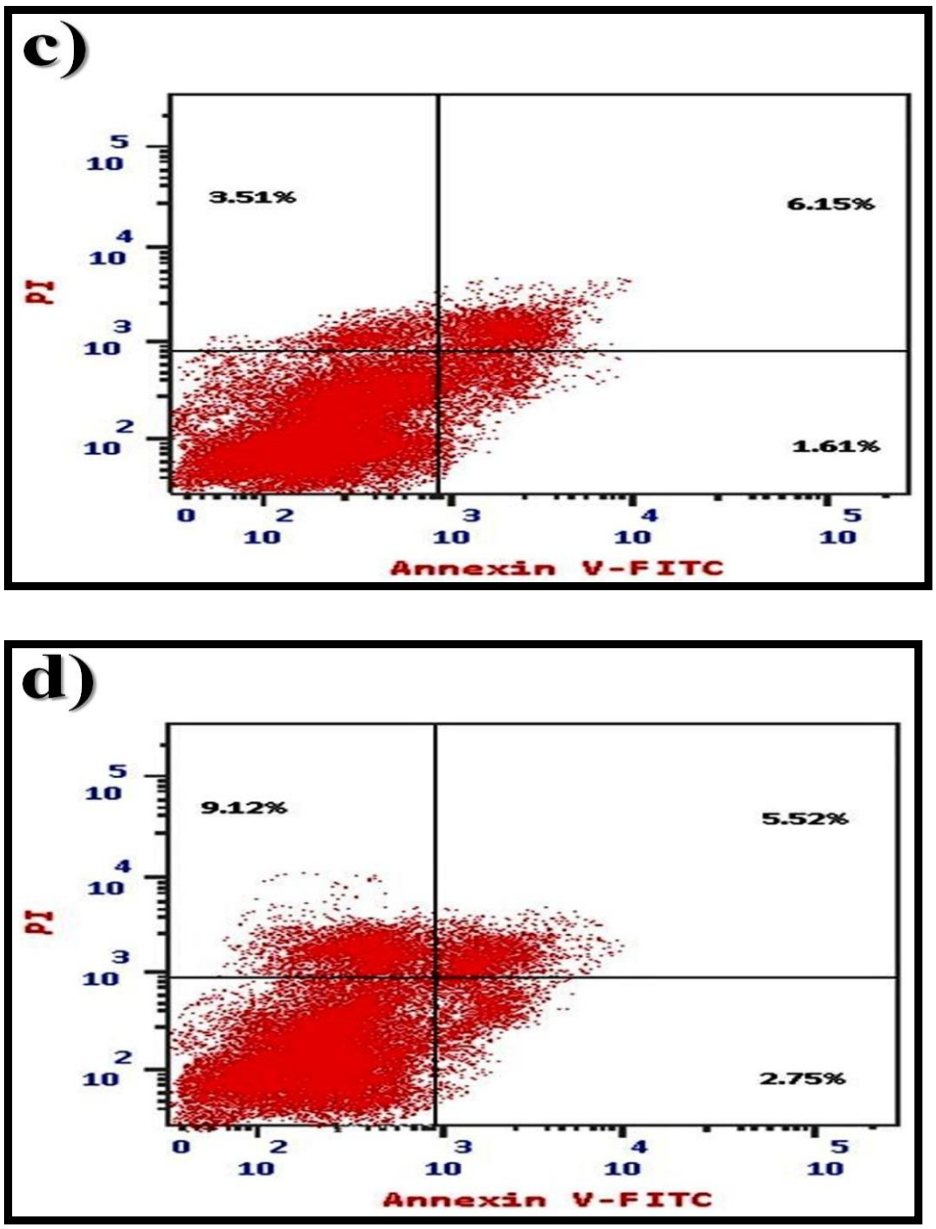

Figure 9: Data of Apoptosis Assay with Annexin V-FITC showing a) Control HepG2, b) HepG2 treated with doxorubicin, c) HepG2 treated with native *S. costus* extract, d) HepG2 treated with gold *S. costus* nano-extract.

3.6. The median lethal dose (LD_{50})

The study aimed to determine the median and therapeutic doses of the native extract and gold nano-extract when administered orally to experimental mice via a stomach tube. Our findings revealed that the presence of biosynthesized Au-NPs increased the safety of the gold nano-extract compared to the native extract alone. Specifically, the LD_{50} and therapeutic doses (1/20 LD_{50}) of the gold nano-extract were higher (11333.33 and 566.67 µg/Kg, respectively) compared to those of the native extract (7333.33 and 366.67 µg/Kg, respectively) **(Fig. 10)**.

4. Discussion

Phenolic compounds are known for their antioxidant and antimicrobial properties, which can promote human health and prevent various diseases **[42]**. In this study, it was found that the methanolic extract had the highest concentrations of polyphenolic compounds and total tannins, followed

by the aqueous extract and then the ethyl acetate extract. This finding is consistent with the suggestion by **Gheraibia et al. [43]** that the concentration of these phenolic compounds depends on the properties of the extracts and the polarity of the solvents used in the extraction process. **Ahmed et al. [44]** also demonstrated that the methanolic extract had the highest antioxidant and reducing properties, which may be attributed to its higher total polyphenolic content compared to the aqueous extract. **Gheraibia et al. [43]** further added that the antioxidant and scavenging properties of the extract are positively influenced by the phenolic content and composition, which can be affected by changing the polarity of the solvents. Therefore, the methanolic extract exhibited stronger activities. The variation in antioxidant and scavenging activities among the different extracts may be due to the differences in reactivity and chemical complexity of the extracts **[45]**. The potent antioxidant activities may also be related to the position of functional groups in the secondary metabolites **[44]** and the presence of specific phytochemicals with electron-donating properties **[46]**. Although the studied extracts showed good antioxidant and scavenging activities, their activities were lower than that of ascorbic acid (standard), which may be attributed to their high proton donating ability **[47]**.

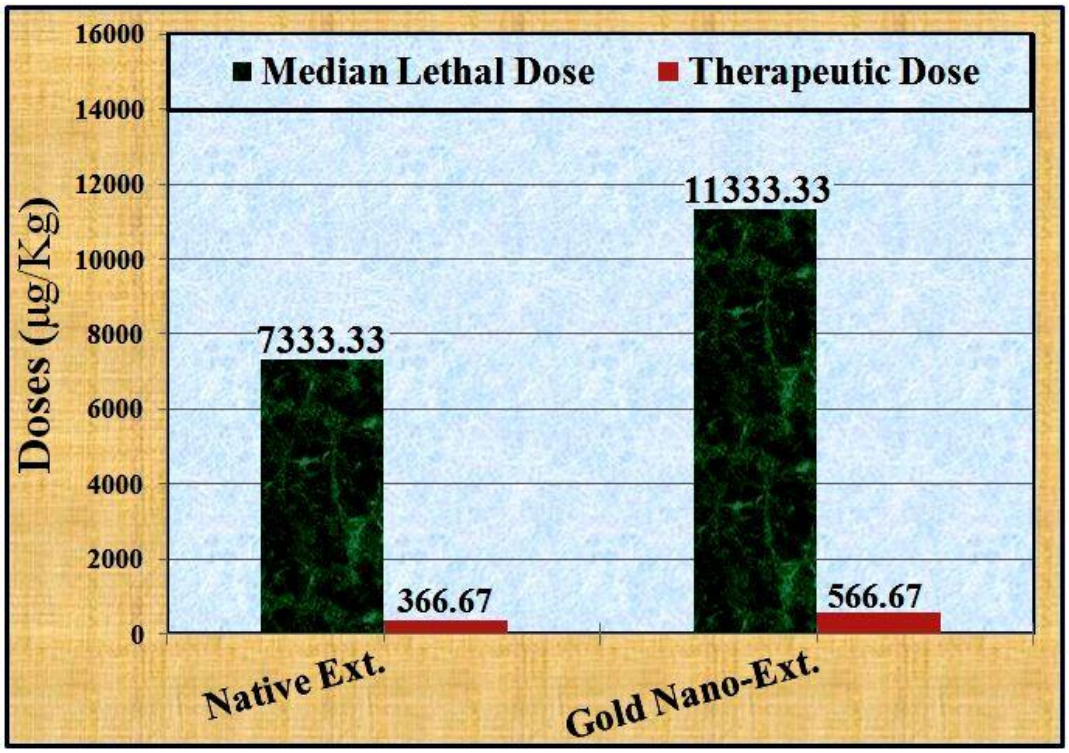

Figure 10: The median lethal (LD_{50}) and therapeutic doses of *S. costus* extract incorporated with Au-NPs and compared to the native one.

Inhibition of α-amylase and α-glucosidase activities delays carbohydrate digestion and glucose absorption, resulting in a decrease in postprandial hyperglycemia **[48]**. The methanolic extract of *S. costus* has the highest inhibitory effect on these enzymes, attributed to the presence of secondary metabolites such as phenolic acids and tannins, which are the main phyto-constituents responsible for its anti-diabetic activity **[49,50]**. However, the inhibitory effect of the studied extracts on these enzyme activities is still lower than that of acarbose (standard), as reported by **Kifle et al. [51]**.

Inhibition of AChE remains the primary therapeutic approach for treating Alzheimer's disease **[52]**. The methanolic extract demonstrated the strongest inhibitory effect on the activity of the AChE enzyme, which aligns with the findings of **Peckels et al. [53]**, who suggested that the inhibition of AChE may be attributed to the high polyphenolic content present. Additionally, **Rauter et al. [54]** stated that there is a positive correlation between AChE inhibition and the total phenolic content of the extract.

Table 5

Data of the EGFR, Bcl2 and Casp3 genes expressed in the HepG2 cells treated with gold *S. costus* nano-extract and compared to those treated with native extract and doxorubicin (as standard drug).

Extract	Conc.	EGFR							
		Control cells			Test cells				FLD
		GAP HC	EG TC	ΔC TC	GAP HE	EG TE	ΔC TE	ΔΔ ΔCTE	2^- Eamp=1.
Native Extract		24.05	27.9	3.6	23.88	27.9	4.0	0.44	0.76
Gold Nano-Doxorubicin		24.05	27.9	3.6	23.49	28.1	4.6	1.06	0.52
		24.05	27.9	3.6	23.77	30.0	6.4	2.88	0.17
Control		24.05	27.9	3.6	24.05	27.9	3.6	0.00	1.00

Extract	Conc.	Bcl2							
		Control cells			Test cells				FLD
		GAP HC	Bc T	ΔC TC-	GAP HE	Bc T	ΔC TE-	ΔΔ CT ΔCTE-	2^- Eamp=1.
Native Extract		24.05	28.1	3.97	23.88	28.1	4.2	0.26	0.85
Gold Nano-Doxorubicin		24.05	28.1	3.97	23.49	28.1	5.3	1.33	0.44
		24.05	28.1	3.97	23.77	28.1	4.8	0.83	0.60
Control		24.05	28.1	3.97	24.05	28.1	3.9	0.00	1.00

Extract	Conc.	Casp-3							
		Control cells			Test cells				FLD
		GAP HC	Ca TC	ΔC TC-	GAP HE	Ca TE	ΔC TE-	ΔΔ CT ΔCTE	2^- Eamp=1.
Native Extract		24.05	33.7	9.8	23.88	32.1	8.7	-1.09	1.95
Gold Nano-Doxorubicin		24.05	33.7	9.8	23.49	31.6	8.1	-1.74	2.92
		24.05	33.7	9.8	23.77	30.2	6.4	-3.46	8.39
Control		24.05	33.7	9.8	24.05	33.7	9.8	0.00	1.00

The methanolic extract exhibited anti-inflammatory activity, which could be attributed to the presence of various phyto-constituents such as alkaloids, flavonoids, carbohydrates, glycosides, saponins, tannins, and phenolic compounds **[55]**.

The cytotoxic activities of *S. costus* extract were evaluated against the growth of cancer cells. The results of the present study showed that the methanolic extract exhibited higher cytotoxic activity with a lower IC_{50} against HepG2 compared to Caco2. This could be attributed to the presence of a mixture of phyto-components that displayed significant anticancer activity with various therapeutic properties, making the extract more effective in treating diseases than individual products **[56]**. Furthermore, the *S. costus* extract was found to decrease the viability of cancer cells by inducing the release of cytochrome C from the mitochondria to the cytosol through apoptotic stimuli **[57]**. **Alotaibi et al. [58]** also reported that the *S. costus* extract is rich in natural anti-hepatic cancer compounds, which exhibited anti-proliferative effects against HepG2 cells. This was attributed to its ability to activate apoptosis, increase early and late apoptosis cell populations, and enhance the permeability of the mitochondrial membrane. These actions ultimately lead to cytochrome C-mediated apoptosis and the up-regulation of apoptosis gene markers.

In the current study, we utilized the methanolic *S. costus* extract to synthesize Au-NPs, which were then characterized using advanced instrumental techniques. The spectral, morphological, and structural data of the synthesized Au-NPs were found to be consistent with the results reported by

Abdel-Halim et al. [59] and further supported by **Aboulthana et al. [60]**.

The size of the biosynthesized Au-NPs is correlated to the percentage of polyphenolic compounds consumed. As the amount of polyphenolic compounds used for their formation increased, the size of the Au-NPs decreased. This finding is consistent with **Mystrioti et al. [61]**, who suggested that the concentration of phenolic compounds increased in the gold *S. costus* nano-extract due to the regeneration of polyphenolic compounds, possibly under the catalytic reaction conditions and/or interference from the small biosynthesized Au-NPs. The increase in total polyphenolic content after the reaction may be attributed to an overestimation of organic compounds present in the extract that are not involved in the reaction with the characteristic Folin-Ciocalteu **[62]**.

The scavenging activity of the methanolic *S. costus* extract was found to increase after the incorporation of Au-NPs, which is consistent with the findings of **Du et al. [63]**. They suggested that the biofabricated Au-NPs are able to transfer electrons or hydrogen to the free radicals at the atomic level. The activity of the biosynthesized Au-NPs is believed to be influenced by their larger surface area, and the scavenging activity of the extract tends to increase with higher concentrations of incorporated Au-NPs, as reported by **Swamy et al. [64]**.

The presence of Au-NPs in the *S. costus* nano-extract enhances its anti-diabetic activity by inhibiting the activities of α-amylase and α-glucosidase enzymes. This finding is consistent with the study conducted by **Govindaraju and Suganya [65]**, who suggested that the biosynthesized Au-NPs could be developed as potent anti-diabetic nanomaterials due to their ability to inhibit the breakdown of starch by metabolic enzymes. The Au-NPs also increase the inhibitory effect of the extract on AChE activity. This may be attributed to the structural perturbation of the enzyme, which is inhibited by its adsorption on the surface of the Au-NPs and subsequent stabilization of the enzyme structure. Additionally, the distribution of surface charge on the AChE enzyme can be altered by inducing H_2S synthesizing enzymes, further contributing to the inhibition of AChE enzyme activity **[66]**. It is worth noting that AChE has a strong affinity to adsorb on Au-NPs, leading to conformational changes and subsequent inactivation of AChE activity **[67]**. The biosynthesized Au-NPs have the ability to stabilize tertiary and quaternary protein structures, which explains their good anti-inflammatory activity. This can be attributed to their inhibitory potential on protein denaturation **[68,69]**.

The presence of Au-NPs in the *S. costus* nano-extract increased cytotoxic activity, which is consistent with the findings of **Mata et al. [70]**. They suggested that the biosynthesized Au-NPs have the potential to act as therapeutic agents for destroying cancer cells. Additionally, the biosynthesized Au-NPs, along with their active constituents, can cause significant morphological changes in cancer cells and inhibit their growth after 48 hours of treatment, as reported by **Khoobchandani et al. [71]**. **Rajkuberan et al. [72]** proposed that the cytotoxic activity induced by biosynthesized Au-NPs is influenced by their size, shape, and the biomolecules grafted onto their surface.

The potential anti-tumor activity of *S. costus* nano-extract can be easily studied by examining its effects on the cell cycle **[73]**. In this study, it was found that the *S. costus* extract demonstrated the ability to induce apoptosis in HepG2 cells. As a result, it caused cell cycle arrest in one of the aforementioned phases. This finding is consistent with the research conducted by **Mans et al. [74]**, who suggested that the *S. costus* extract possesses a strong anticancer effect by promoting apoptosis in cancer cells. The temporary or permanent arrest of the cell cycle at the **S** phase, which occurs during DNA replication, may be attributed to the regulation of the cell cycle through the Akt signaling pathway, Cdk2, Cyclin A, and Cyclin E **[75]**.

The Bcl2 protein is part of a large family of proteins that regulate apoptosis through the mitochondrial pathway **[76]**. The gold nano-extract altered the expression of the EGFR, Bcl2, and Casp3 genes in HepG2 cells compared to cells treated with the native extract or control HepG2 cells. This suggests that the presence of Au-NPs disrupted signal transduction pathways, leading to an overproduction of reactive oxygen species (ROS) and ultimately enhancing cellular death **[77]**. Additionally, the gold nano-extract significantly increased the percentage of total, early, and late apoptotic cells, as well as necrosis, in HepG2 cells

compared to the cells treated with the native extract or control HepG2 cells. This could be attributed to the wide range of phyto-constituents present in the extract, which play a crucial role in regulating apoptosis and inhibiting the growth of cancer cells **[78]**. **Singireesu et al. [79]** demonstrated that the extract-induced apoptosis in HepG2 cells may involve the mitochondrial-mediated caspase activation pathway. Furthermore, the presence of M-NPs in the nano-extract stimulated apoptosis by increasing the excessive generation of ROS, which inhibited cellular replication **[80]**.

No toxicity was observed when the gold *S. costus* nano-extract was administered orally to mice. In fact, it was found to be safer than the native extract itself. As a result, the LD_{50} of the gold nano-extract was higher than that of the native extract. This finding is consistent with the research conducted by **Aboulthana et al. [60]** and has been further supported by **Bekheit et al. [81]**. These studies suggest that the safety of the gold nano-extract may be attributed to the efficiency of the urinary excretory system in eliminating the M-NPs from the body through tubular secretion and glomerular filtration. Additionally, the low degradation rate of the gold nano-extract further minimizes the risk of potential side effects.

5. Conclusion

The methanolic extract of *S. costus* is abundant in major phyto-constituents and showed the most significant *in vitro* biological activities compared to the other extracts (aqueous, methanol, and ethyl acetate). As a result, it was selected for the biosynthesis of Au-NPs. The Gold Nano-Extract of *Saussurea costus* exhibited greater antioxidant, anti-diabetic, anti-Alzheimer, anti-inflammatory, and cytotoxic properties compared to the original extract. Additionally, the gold nano-extract was found to be safer than the native extract when administered orally to mice.

Acknowledgments

The authors would like to express their gratitude to the National Research Centre in Dokki, Giza, Egypt for their invaluable technical support and provision of facilities, which greatly contributed to the successful completion of this research project.

Author contributions

WMA, AGH, and MMA proposed the idea and gathered relevant previously published papers. They also designed the experimental work. AAF and AHA were responsible for preparing the plant extract. AMY focused on the biosynthesis of Au-NPs using the plant extract. WMA, AGH, and MMA conducted the molecular experiments. All authors approved the final draft of the manuscript. WMA communicated with journal editors to request publication of the manuscript.

Conflict of interest

The authors have stated that there are no financial or non-financial conflicts of interest among them.

Ethical approval

The experimental design was conducted following the protocol published in the "Guide for the Care and Use of Laboratory Animals" and approved by the Institutional Animal Ethics Committee of the National Research Centre, located in Dokki, Giza, Egypt.

References

[1] Abdallah, E.M. Plants: An alternative source for antimicrobials. *J. Appl. Pharm. Sci.*, **1**, 16-20 (2011).

[2] Altwaijry, N.; El-Masry, T.A.; Alotaibi, B.; Tousson, E. and Saleh, A. Therapeutic Effects of Rocket Seeds (*Eruca sativa* L.) against Testicular Toxicity and Oxidative Stress Caused by Silver Nanoparticles Injection in Rats. *Environ. Toxicol.*, **35**(9), 952-960 (2020).

[3] Pandey, M.M.; Rastogi, S. and Rawat, A.K.S. *Saussurea costus*: botanical, chemical and pharmacological review of an ayurvedic medicinal plant. *J Ethnopharmacol*., **110**(3), 379-390 (2007).

[4] Tousson, E.; El-Atrsh, A.; Mansour, M. and Abdallah, A. Modulatory Effects of *Saussurea Lappa* Root Aqueous Extract against Ethephon-induced Kidney Toxicity in Male Rats. *Environ. Toxicol*., 34(12), 1277-1284 (2019).

[5] Tousson, E.; Hafez, E.; Abo Gazia, M.M.; Salem, S.B. and Mutar, T.F. Hepatic Ameliorative Role of Vitamin B17 against Ehrlich Ascites Carcinoma-Induced Liver Toxicity. Environ. Sci. Pollut. Res., **27**, 9236-9246 (2020).

[6] Ansari, S.; Siddiqui, M.; Malhotra, S. and Maaz, M. Antiviral Efficacy of Qust (*Saussurea lappa*) and Afsanteen (*Artemisia absinthium*) for Chronic Hepatitis B: A Prospective Single-Arm Pilot Clinical Trial. Pharmacogn. Res., **10**, 282 (2018).

[7] Hassan, R. and Masoodi, M.H. *Saussurea lappa*: A comprehensive review on its pharmacological activity and phytochemistry. *Curr. Tradit. Med*., **6**, 13-23 (2020).

[8] Ghasham, A.A.; Muzaini, M.A.; Qureshi, K.A.; Elhassan, G.O.; Khan, R.A.; Farhana, S.A.; Hashmi, S.; El-Agamy, E. and Abdallah, W.E. Phytochemical Screening, Antioxidant and Antimicrobial Activities of Methanolic Extract of *Ziziphus mauritiana* Lam. Leaves Collected from Unaizah, Saudi Arabia. Int. J. Pharm. Res. Allied Sci., **6**, 33-46 (2017).

[9] Nadda, R.K.; Ali, A.; Goyal, R.C.; Khosla, P.K. and Goyal, R. Aucklandia costus (Syn. *Saussurea costus*): Ethnopharmacology of an Endangered Medicinal Plant of the Himalayan Region. *J. Ethnopharmacology*, **263**, 113199 (2020).

[10] Ravinder, S. and Khushminder, K. Phytochemical analysis and *in vitro* antioxidant capacity of different solvent extracts of *Saussurea lappa* L. roots. *Journal of Pharmacognosy and Phytochemistry*, **7**, 427-432 (2018).

[11] Guldiken, B.; Ozkan, G.; Catalkaya, G.; Ceylan, F.D.; Yalcinkaya, I.E. and Capanoglu, E. Phytochemicals of herbs and spices: Health versus toxicological effects. *Food Chem. Toxicol*., **119**, 37-49 (2018).

[12] Deabes, M.M.; Aboulthana, W.M.; Marzouk, E.M.A.; Mohamed, M.I. and Ahmed, K.A. Evaluation of Hepato- and Neuroprotective Effect of Chemical Constituents in *Saussurea costus* Extract against the Toxicity Induced by Chloropyrifos Ethyl in Rats. *Egyptian Journal of Chemistry*, **64**(2), 631-647 (2021).

[13] Shibata, M.; Ogawa, T. and Kawashita, M. Synthesis of iron nitride nanoparticles from magnetite nanoparticles of different sizes for application to magnetic hyperthermia. *Ceramics International*, **45**(17, Part B), 23707-23714 (2019).

[14] Fatimah, Pratiwi, E.Z. and Wicaksono, W.P. Synthesis of magnetic nanoparticles using Parkia speciosa Hassk pod extract and photocatalytic activity for Bromophenol blue degradation. *The Egyptian Journal of Aquatic Research*, **46**(1), 35-40 (2020).

[15] Gunarani, G.I.; Raman, A.B.; Kumar, J.D.; Natarajan, S. and Jegadeesan, G.B. Biogenic synthesis of Fe and NiFe nanoparticles using *Terminalia bellirica* extracts for water treatment applications. *Materials Letters*, **247**, 90-94 (2019).

[16] Meenakshisundaram, S.; Krishnamoorthy, V.; Jagadeesan, Y.; Vilwanathan, R. and Balaiah, A. *Annona muricata* assisted biogenic synthesis of silver nanoparticles regulates cell cycle arrest in NSCLC cell lines. *Bioorganic Chemistry*, 95, 103451 (2020).

[17] Aygün, A.; Gülbağça, F.; Nas, M.S.; Alma, M.H.; Çalımlı, M.H.; Ustaoglu, B.; Altunoglu, Y.C.; Baloğlu, M.C.; Cellat, K. and Şen, F. Biological synthesis of silver nanoparticles using Rheum ribes and evaluation of their anticarcinogenic and antimicrobial potential: A novel approach in phytonanotechnology. *Journal of Pharmaceutical and Biomedical Analysis*, **179**: 113012 (2020).

[18] Kiran, V.S. and Sumathi, S. Comparison of catalytic activity of bismuth substituted cobalt ferrite nanoparticles synthesized by combustion and co-precipitation method. J. Magn. Magn. Mater., **421**, 113-119 (2017).

[19] Ragupathi, C.; Vijaya, J.J. and Narayanan, S. Catalytic properties of nanosized zinc aluminates prepared by green process using *Opuntia dilenii* haw plant extract. Chin. J. Catal., **34**(10), 1951-1958 (2013).

[20] Surendra, T.V.; Roopan, S.M. and Arasu, M.V. RSM optimized *Moringa oleifera* peel extract for green synthesis of *M. oleifera* capped palladium nanoparticles with antibacterial and hemolytic property. J. Photochem. Photobiol. B Biol., **162**, 550-557 (2016).

[21] Suppi, S.; Kasemets, K.; Ivask, A.; Künnis-Beres, K.; Sihtmäe, M.; Kurvet, I.; Aruoja, V. and Kahru, A. A novel method for comparison of biocidal properties of nanomaterials to bacteria, yeasts and algae. *J. Hazard Mater*., **286**, 75-84 (2015).

[22] Munk, M.; Brandão, H.M.; Nowak, S.; Mouton, L.; Gern, J.C.; Guimaraes, A.S.; Yéprémian, C.; Couté, A.; Raposo, N.R.; Marconcini, J.M. and Brayner, R. Direct and indirect toxic effects of cotton-derived cellulose nanofibres on filamentous green algae. *Ecotoxicol. Environ. Saf*., **122**, 399-405 (2015).

[23] Akhtar, M.S.; Bashir, S.; Malik, M. and Manzoor, R. Cardiotonic activity of methanolic extract of *Saussurea lappa* Linn roots. *Pak. J. Pharm. Sci*., **26**(6), 1197-1201 (2013).

[24] Singleton, V.L. and Rossi, J.A. Colorimetry of total phenolics with phosphomolybdicphosphotungstic acid reagents. *Am. J. Enol. Vitic*., **16**(3), 144-158 (1965).

[25] Broadhurst, R.B. and Jones, W.T. Analysis of condensed tannins using acidified vanillin. *Journal of the Science of Food and Agriculture*, **48**(3), 788-794 (1978).

[26] Prieto, P.; Pineda, M. and Aguilar, M. Spectrophotometric quantitation of antioxidant capacity through the formation of a phosphomolybdenum complex: Specific application to the determination of vitamin E. *Anal. Biochem*., **269**, 337-341 (1999).

[27] Oyaizu, M. Studies on product of browning reaction prepared from glucose amine. *Japanese Journal of Nutrition*, **44**, 307-315 (1986).

[28] Rahman, M.M.; Islam, M.B.; Biswas, M. and Alam, A.K. *In vitro* antioxidant and free radical scavenging activity of different parts of *Tabebuia pallida* growing in Bangladesh. *BMC Research Notes*, **8**(1), 621-628 (2015).

[29] Arnao, M.B.; Cano, A. and Acosta, M. The hydrophilic and lipophilic contribution to total antioxidant activity. *Food Chem*., **73**, 239-244 (2001).

[30] Wickramaratne, M.N.; Punchihewa, J. and Wickramaratne, D. *In-vitro* alpha amylase inhibitory activity of the leaf extracts of *Adenanthera pavonina*. *BMC Complement. Altern. Med*., **16**(1), 466 (2016).

[31] Pistia-Brueggeman, G. and Hollingsworth, R.I. A preparation and screening strategy for glycosidase inhibitors. *Tetrahedron*, **57**, 8773-8778 (2001).

[32] Ellman, G.L.; Courtney, K.D.; Andres, V.J. and Featherstone, R.M. A new and rapid colorimetric determination of acetylcholinesterase activity. *Biochem. Pharmacol*., **7**, 88-95 (1961).

[33] Das, S. and Sureshkumar, P. Effect of methanolic root extract of *Blepharispermum subsesssile* DC in controlling arthritic activity. *Research Journal of Biotechnology*, **11**(4), 65-74 (2016).

[34] Oyedapo, O.O. and Famurewa, A.J. Antiprotease and Membrane Stabilizing Activities of Extracts of Fagara Zanthoxyloides, Olax Subscorpioides and Tetrapleura Tetraptera. *Int. J. Pharmacogn*., **33**(1), 65-69 (1995).

[35] Meera, S.; Ramaiah, N. and Kalidindi, N. Illustration of anti-rheumatic mechanism of rheumavedic capsule. *Saudi Pharm. J.*, **19**(4), 279-284 (2011).

[36] Vichai, V. and Kirtikar, K. Sulforhodamine B colorimetric assay for cytotoxicity screening. *Nature Protocols*, **1**(3), 1112-1116 (2006).

[37] Pfaffl, M.W. A new mathematical model for relative quantification in real-time RT–PCR. *Nucleic Acids Research*, **29**, e45-e45 (2001).

[38] Wang, J.; Deng, X.; Zhang, F.; Chen, D. and Ding, W. ZnO nanoparticle-induced oxidative stress triggers apoptosis by activating JNK signaling pathway in cultured primary astrocytes. *Nanoscale Research Letters*, **9**(1), 1-12 (2014).

[39] Koopman, G.; Reutelingsperger, C.P.; Kuijten, G.A.; Keehnen, R.M.; Pals, S.T. and Van Oers, M.H. Annexin V for flow cytometric detection of phosphatidylserine expression on B cells undergoing apoptosis. *Blood*, **84**(5), 1415-1420 (1994).

[40] Zhao, P.; Li, N. and Astruc, D. State of the art in gold nanoparticle synthesis. *Coord. Chem. Rev*., **257**(3-4), 638-665 (2013).

[41] Paget, G.E. and Barnes, J.M. Toxicity tests. In: Laurance DR, Bacharach AL, editors. Evaluation of Drug Activities: Pharmacometrics, Vol 1. New York: Academic Press: p. 135-65 (1964).

[42] Tungmunnithum, D.; Thongboonyou, A.; Pholboon, A. and Yangsabai, A. Flavonoids and other phenolic compounds from medicinal plants for pharmaceutical and medical aspects: an overview. *Medicine*, **5**(3), 93 (2018).

[43] Gheraibia, S.; Belattar, N. and Abdel-Wahhab, M.A. HPLC analysis, antioxidant and cytotoxic activity of different extracts of *Costus speciosus* against HePG-2 cell lines. *South Afr. J. Bot*., **131**, 222-228 (2020).

[44] Ahmed, A.; Ahmad, S.; Soni, K.; Lapa, B.; Af zal, M.; Sharma, K. and Kumar, G. Suitable solvent and drying condition to enhance phenolics and extractive value of *Saussurea costus*. J. Ayurveda Holist. Med., **2**(5), 165-170 (2016).

[45] El-Far, A.H.; Shaheen, H.M.; Alsenosy, A.W.; El-Sayed, Y.S.; Al Jaouni, S.K. and Mousa, S.A. *Costus speciosus*: traditional uses, phytochemistry, and therapeutic potentials. Phcog. Rev., **12**(23), 120-127 (2018).

[46] Balasundram, N.; Sundram, K. and Samman, S. Phenolic compounds in plants and agri-industrial by-products: antioxidant activity, occurrence, and potential uses. *Food Chem*., **99**(1), 191-203 (2006).

[47] Hassan, A.S.; Morsy, N.M.; Aboulthana, W.M. and Ragab, A. Exploring novel derivatives of isatin-based Schiff bases as multi-target agents: design, synthesis, in vitro biological evaluation, and in silico ADMET analysis with molecular modeling simulations. *RSC Advances*, **13**(14), 9281-9303(2023).

[48] Hassan, A.S.; Morsy, N.M.; Aboulthana, W.M. and Ragab, A. *In vitro* enzymatic evaluation of some pyrazolo[1,5-a] pyrimidine derivatives: Design, synthesis, antioxidant, anti-diabetic, anti-Alzheimer, and anti-arthritic activities with molecular modeling simulation. *Drug Development Research*, **84**(1), 3-24 (2023).

[49] Karakaya, S.; Gözcü, S.; Güvenalp, Z.; Özbek, H.; Yuca, H.; Dursunoğlu, B.; Kazaz, C. and Kılıç, C.S. The α-amylase and α-glucosidase inhibitory activities of the dichloromethane extracts and constituents of *Ferulago bracteata* roots. *Pharm. Biol*., **56**(1), 18-24 (2018).

[50] Kifle, Z.D.; Kidanu, B.B.; Tadesse, T.Y.; Belachew, T.F. and Atnafie, S.A. Evaluation of *in vivo* antidiarrheal activity of solvent fractions of *Hagenia abyssinica* (*Rosaceae*) in Swiss albino mice. *Evidence-based Complementary and Alternative Medicine* Volume 2021, Article ID 8828331, 9 Pages (2021a).

[51] Kifle, Z.D.; Debeb, S.G. and Belayneh, Y.M. *In Vitro* α-Amylase and α-Glucosidase Inhibitory and Antioxidant Activities of the Crude Extract and Solvent Fractions of *Hagenia abyssinica* Leaves. *BioMed Research International* Volume 2021, Article ID 6652777, 9 Pages (2021b).

[52] Alkahtani, H.M.; Almehizia, A.A.; Al-Omar, M.A.; Obaidullah, A.J.; Zen, A.A.; Hassan, A.S. and Aboulthana, W.M. *In Vitro* Evaluation and Bioinformatics Analysis of Schiff Bases Bearing Pyrazole Scaffold as Bioactive Agents: Antioxidant, Anti-Diabetic, Anti-Alzheimer, and Anti-Arthritic. *Molecules*, **28**(20), 7125 (2023).

[53] Peckels, C.M.; Alexander, N.S.; Wilson, G.N.; Karty, J.M. and Matera, K.M. Trisubstituted phenolic compounds as inhibitors of acetylcholinesterase and amyloid beta aggregate formation. *Curr. Enz. Inhibition*, **9**, 67-74 (2013).

[54] Hassan, A.S. and Aboulthana, W.M. Synthesis, *In Vitro* Biological Investigation, and In Silico Analysis of Pyrazole-Based Derivatives as Multi-target Agents. *Egyptian Journal of Chemistry*, **66**(6), 441-455 (2023).

[55] Chandur, U.; Shashidhar, S.; Chandrasek, S.B.; Bhanumathy, M. and Midhun, T. Phytochemical Evaluation and Anti-Arthritic Activity of Root of *Saussurea lappa*. *Pharmacologia*, **2**(9), 265-267 (2011).

[56] Tian, X.; Song, H.S.; Cho, Y.M.; Park, B.; Song, Y.J.; Jang, S. and Kang, S.C. Anticancer effect of *Saussurea lappa* extract *via* dual control of apoptosis and autophagy in prostate cancer cells. *Medicine*, **96**, e7606 (2017).

[57] Shati, A.A.; Alkahtani, M.A.; Alfaifi, M.Y.; Elbehairi, S.E.I.; Elsaid, F.G.; Prasanna, R. and Mir, M.A. Secondary Metabolites of *Saussurea costus* Leaf Extract Induce Apoptosis in Breast, Liver, and Colon Cancer Cells by Caspase-3-Dependent Intrinsic

Pathway. *BioMed Res. Int.,* Volume 2020, Article ID 1608942 (2020).

[58] Alotaibi, A.A.; Bepari, A.; Assiri, R.A.; Niazi, S.K.; Nayaka, S.; Rudrappa, M.; Nagaraja, S.K. and Bhat, M.P. *Saussurea lappa* Exhibits Anti-Oncogenic Effect in Hepatocellular Carcinoma, HepG2 Cancer Cell Line by Bcl-2 Mediated Apoptotic Pathway and Mitochondrial Cytochrome C Release. *Curr. Issues Mol. Biol*., **43**(2), 1114-1132 (2021).

[59] Abdel-Halim, A.H.; Fyiad, A.A.; Aboulthana, W.M.; El-Sammad, N.M.; Youssef, A.M. and Ali, M.M. Assessment of the Anti-diabetic Effect of *Bauhinia variegata* Gold Nano-Extract against Streptozotocin Induced Diabetes Mellitus in Rats. *Journal of Applied Pharmaceutical Science*, **10**(05), 077-091 (2020).

[60] Aboulthana, W.M.K.; Refaat, E.; Khaled, S.E.; Ibrahim, N.E. and Youssef, A.M. Metabolite Profiling and Biological Activity Assessment of *Casuarina equisetifolia* Bark after Incorporating Gold Nanoparticles. *Asian Pacific Journal of Cancer Prevention*, **23**(10): 3457-3471 (2022).

[61] Mystrioti, C.; Xanthopoulou, T.D.; Tsakiridis, P.E.; Papassiopi, N. and Xenidis, A. Comparative evaluation of five plant extracts and juices for nanoiron synthesis and application for hexavalent chromium reduction. *Sci. Total Environ*., **539**, 105-113 (2016).

[62] Alegria, E.C.B.A.; Ribeiro, A.P.C.; Mendes, M.; Ferraria, A.M.; do Rego, A.M.B. and Pombeiro, A.J.L. Effect of Phenolic Compounds on the Synthesis of Gold Nanoparticles and its Catalytic Activity in the Reduction of Nitro Compounds. Nanomaterials (Basel), **8**(5), 320 (2018).

[63] Du, L.; Suo, S.; Wang, G.; Jia, H.; Liu, K.J.; Zhao, B. and Liu, Y. Mechanism and cellular kinetic studies of the enhancement of antioxidant activity by using surface-functionalized gold nanoparticles. *Chem. Eur. J.*, **19**, 1281-1287 (2013).

[64] Swamy, M.K.; Akhtar, M.S.; Mohanty, S.K. and Sinniah, U.R. Synthesis and characterization of silver nanoparticles using fruit extract of *Momordica cymbalaria* and assessment of their in vitro antimicrobial, antioxidant and cytotoxicity activities. *Spectrochim Acta. A*, **151**, 939-944 (2015).

[65] Govindaraju, K. and Suganya, K.S.U. *In vitro* anti-diabetic assessment of guavanoic acid functionalized gold nanoparticles in regulating glucose transport using L6 rat skeletal muscle cells. *RSC Med. Chem.*, **11**(7), 814-822 (2020).

[66] El-Feky, A. and Aboulthana, W. Chemical composition of lipoidal and flavonoidal extracts from Egyptian olive leaves with *in vitro* biological activities. Egyptian Journal of Chemistry, **66**(SI 13), 1903-1913 (2023).

[67] Hou, K.; Zhao, J.; Wang, H.; Li, B.; Li, K.; Shi, X.; Wan, K.; Ai, J.; Lv, J.; Wang, D.; Huang, Q.; Wang, H.; Cao, Q.; Liu, S. and Tang, Z. Chiral gold nanoparticles enantioselectively rescue memory deficits in a mouse model of Alzheimer's disease. *Nat. Commun*., **11**(1), 4790 (2020).

[68] Prabakaran, A.S. and Mani, N. Anti-inflammatory activity of silver nanoparticles synthesized from *Eichhornia crassipes*: An *in vitro* study. *J. Pharmacogn. Phytochem*., **8**(4), 2556-2558 (2019).

[69] Azeem, M.N.A.; Ahmed, O.M.; Shaban, M. and Elsayed, K.N. *In vitro* antioxidant, anticancer, anti-inflammatory, anti-diabetic and anti-Alzheimer potentials of innovative macroalgae bio-capped silver nanoparticles. *Environ. Sci. Pollut. Res*., **29**(39), 59930-59947 (2022).

[70] Mata, R.; Nakkala, J.R. and Sadras, S.R. Polyphenol stabilized colloidal gold nanoparticles from *Abutilon indicum* leaf extract induces apoptosis in HT-29 colon cancer cells. *Colloids Surf B*, 143, 499-510 (2016).

[71] Khoobchandani, M.; Zambre, A.; Katti, K.B.S. ; Lin, C.H. and Katti, K.V. Green nanotechnology from brassicaceae development of broccoli phytochemicals-encapsulated gold nanoparticles and their applications in nanomedicine. *Int. J. Green Nanotechnol*., **5**(1), 1-15 (2013).

[72] Rajkuberan, C.; Susha, K.; Sathishkumar, G. and Sivaramakrishnan, S. Antibacterial and cytotoxic potential of silver nanoparticles

synthesized using latex of *Calotropis gigantea* L. *Spectrochim Acta A*, 136, 926-930 (2015).

[73] Evan, G.I. and Vousden, K.H. Proliferation, cell cycle and apoptosis in cancer. *Nature*, 411, 342-348 (2001).

[74] Mans, D.R.A.; Rocha, A.B. and Schwartsmann, G. Anti-cancer drug discovery and development in Brazil: targeted plant collection as a rational strategy to acquire candidate anti-cancer compounds. *The Oncologist*, **5**(3), 185-198 (2000).

[75] Chen, K.C.; Yang, T.Y.; Wu, C.C.; Cheng, C.C.; Hsu, S.L.; Hung, H.W.; Chen, J.W. and Chang, G.C. Pemetrexed induces S-phase arrest and apoptosis via a deregulated activation of Akt signaling pathway. *PLoS ONE*, **9**, e97888 (2014).

[76] Frenzel, A.; Grespi, F.; Chmelewskij, W. and Villunger, A. Bcl2 family proteins in carcinogenesis and the treatment of cancer. *Apoptosis : an International Journal on Programmed Cell Death*, 14(4), 584-596 (2009).

[77] Ismail, E.H.; Saqer, A.; Assirey, E.; Naqvi, A. and Okasha, R. Successful green synthesis of gold nanoparticles using a *Corchorus olitorius* extract and their antiproliferative effect in cancer cells. *International Journal of Molecular Sciences*, **19**(9), 2612 (2018).

[78] Srivastava, A.; Akoh, C.C.; Fischer, J. and Krewer, G. Effect of anthocyanin fractions from selected cultivars of Georgia-grown blueberries on apoptosis and phase II enzymes. *Journal of Agricultural and Food Chemistry*, **55**(8), 3180-3185 (2007).

[79] Hassan, A.S.; Moustafa, G.O.; Awad, H.M.; Nossier, E.S. and Mady, M.F. Design, Synthesis, Anticancer Evaluation, Enzymatic Assays, and a Molecular Modeling Study of Novel Pyrazole−Indole Hybrids. ACS Omega, **6**, 12361-12374 (2021).

[80] Vasanth, K.; Ilango, K.; MohanKumar, R.; Agrawal, A. and Dubey, G.P. Anticancer activity of *Moringa oleifera* mediated silver nanoparticles on human cervical carcinoma cells by apoptosis induction. *Colloids Surf B Biointerfaces*, **117**, 354-359 (2014).

[81] Bekheit, R.A.; Aboulthana, W.M. and Serag, W.M. Bio- and Phyto-chemical Study on *Nannochloropsis oculata* algal Extract Incorporated with Gold Nanoparticles, *in Vitro* Study. *Frontiers in Scientific Research and Technology*, **5**(1), 1-17 (2023).